Ministry of Education
National University of Science and Technology
POLITEHNICA *Bucharest*
Doctoral School Chemical Engineering and Biotechnologies

PhD Thesis Abstract

Decision No…… from …….. 2024

Recuperative separation by composite membranes of the compounds involving olfactory discomfort

Separarea recuperativa prin membrane compozite a compușilor care implică disconfort olfactiv

PhD Student: **Andreia PÎRȚAC**

Supervisor:

***Prof. dr. Eng.* Gheorghe NECHIFOR**

2024, Bucharest

Ministry of Education
National University of Science and Technology
POLITEHNICA *Bucharest*
Doctoral School Chemical Engineering and Biotechnologies

PhD Thesis

Decision No…… from …….. 2024

Recuperative separation by composite membranes of the compounds involving olfactory discomfort

Separarea recuperativa prin membrane compozite a compușilor care implică disconfort olfactiv

PhD Student: **Andreia PÎRȚAC**

PhD THESIS COMMITTEE

President	**Prof. Hab. Dr. Eng. Ștefan Ioan VOICU**	from	**National University of Sciences and Technology Politehnica Bucharest**
Supervisor	**Prof. Dr. Eng. Gheorghe NECHIFOR**	from	**National University of Sciences and Technology Politehnica Bucharest**
Member	**Prof. Dr. Eng. Ioan MAMALIGA**	from	**Gheorghe Asachi University from Iasi**
Member	**Prof. Dr. Rodica Mariana ION**	from	**Valahia University from Târgoviște**
Member	**Prof. Dr. Eng. Gabriel Lucian RADU**	from	**National University of Sciences and Technology Politehnica Bucharest**

2024, Bucharest

CONTENT

INTRODUCTION

Industrial production generates solid, liquid and gaseous, toxic and/or foul-smelling pollutants. In order to solve this environmental problem, various methods of retaining the specific pollutant were used at the source.

Among the non-conventional separation processes for the retention or removal of pollutants from liquid or gaseous media, membranes and membrane techniques can be mentioned.

The main types of membranes are liquid or solid, homogeneous or composite.

The doctoral thesis "Recuperative separation by composite membranes of the compounds involving olfactory discomfort" deals with the recuperative separation of some compounds that generate olfactory discomfort using composite membranes.

Basically, phenolic nitro derivative compounds, from a source phase, are catalytically reduced with molecular hydrogen, using membranes containing osmium nanoparticles, to the aromatic amine of the problem, and the amine is separated through the membrane into a receiving phase.

As target substances, p-nitrophenol and hydrogen sulfide were used, which are toxic and generate olfactory discomfort.

Nitrophenol is used on a large scale mainly in the industry of dyes, pesticides and pharmaceutical compounds, being able to reach the air. The various industrial wastes containing p-nitrophenol are incinerated in thermal power plants, but also in the co-incineration of the cement factory. Incineration produces unwanted nitrogen oxides in the environment. For this

reason, but also because p-nitrophenol has a bad smell, its recuperative separation is recommended.

The importance and method of hydrogen sulfide separation is presented in the dedicated chapter.

The doctoral thesis "Recuperative separation by composite membranes of the compounds involving olfactory discomfort" comprises three parts:

- Part A - literature data synthesis
- Part B – the original research on the recuperative separation of p-nitrophenol
- Part C- general conclusions, originality and research perspectives

The general objective of the doctoral thesis "Recuperative separation by composite membranes of the compounds involving olfactory discomfort" is the design of membranes and membrane systems for the removing of p-nitrophenol and hydrogen sulfide which generating olfactory discomfort and its recovery.

The specific objectives are:

- Obtaining liquid membranes with osmium nanoparticles
- Preparation of polymeric membranes containing osmium nanoparticles
- Obtaining osmium membrane-nanoparticle composite membranes
- Characterization of the obtained membranes
    - o Scanning electron microscopy (SEM)
    - o Energy dispersive X-ray analysis (EDAX)
    - o Thermo-gravimetric and differential scanning thermal analysis (TG, DSC)
    - o Fourier transform infrared spectroscopy (FTIR)
    - o Spectrometry in the ultraviolet and visible range (UV-Vis)
    - o Dynamic Light Scattering (DLS) analysis.
- Determining the performances of the recuperative separation process.

PART A. Synthesis of the literature data

CHAPTER 1.

1.1. Introduction

The reactions of interest for this study can be considered particular cases of a general equilibrium with particle transfer of the type [1-3], relation (1.1) and Figure 1.1:

$$\text{Donor} \rightleftharpoons \text{Acceptor} + \pi \qquad (1.1)$$

The transferred particle (π) can be:

- proton in the case of acid-base balances
- electron in the case of redox balances
- ion or molecule in the case of complexation equilibria

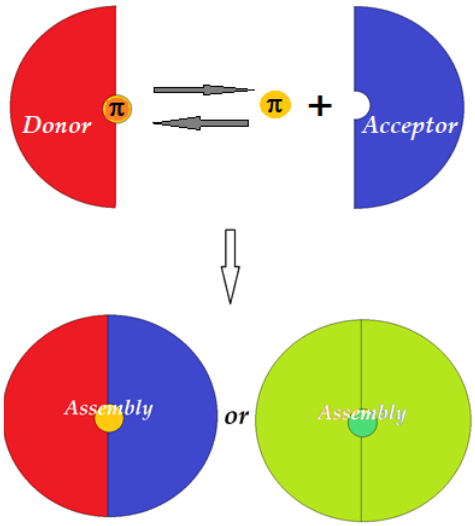

Figure 1.1. Schematic presentation of general equilibrium donor-acceptor in homogeneous system: π-transferable chemical species.

As indicated in figure 1.1, the chemical species that transfer the particle (π) can lead to a molecular assembly in which the donor and acceptor parts retain their structural and

functional identity, or they can lead to a molecular assembly with completely new properties [4,5].

What is essential for the present study, in the interpretation of the transfer, is that the particle (π) cannot exist free in the aqueous solution unless it is an ion or a molecule [6].

In the case of the proton and the electron, the equilibrium considered is mediated by the solvent (water) and accelerated by a catalyst, most often an insoluble material in the working environment, which in this case becomes heterogeneous (Figure 1.2).

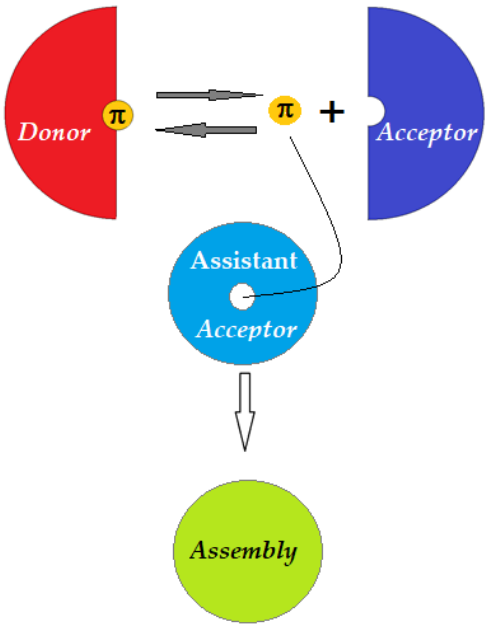

Figure 1.2. Schematic presentation of equilibrium donor acceptor assisted.

These considerations highlight the correlation between acid and base:

$$\underset{\text{(donor)}}{\text{Acid}} \rightleftharpoons \underset{\text{(acceptor)}}{\text{Base}} + H^+ \qquad (1.2)$$

and the most famous and important balance of this kind takes place in water:

$$HOH \rightleftharpoons H^+ + HO^- \qquad (1.3)$$

or since protons cannot exist in a free state, we write the balance (4) with the specific constant (1.4 and 1.5):

$$HOH + (HOH) \rightleftharpoons H^+(HOH) + HO^- \qquad (1.4)$$

$$K = \frac{[HO^-][H_3O^+]}{[HOH]^2} \quad (1.5)$$

where K is the equilibrium constant.

Water being in excess, equation 1.5 is written in the form of a product (1.6)

$$[HO^-][H_3O^+] = K[HOH]^2 = K_w = 10^{-14} \quad (1.6)$$

where Kw is called the ionic product of water.

From a practical point of view, instead of the concentrations of H3O+ and HO-, the co-logarithms (*p*) of these quantities are used, namely:

$$-\log[H_3O^+] = pH \text{ și } -\log[HO^-] = pOH \quad (1.7)$$

In the case of reducers and oxidizers, based on a similar reasoning, but this time the electron being particularly transferred, the relations (1.8-1.11) are obtained:

Considering the redox reaction:

$$Red_1 + Ox_2 \rightleftharpoons Ox_1 + Red_2 \quad (1.8)$$

With equilibrium constant:

$$K = \frac{[Ox_1][Red_2]}{[Red_1][Ox_2]} = \frac{K_1}{K_2} \quad (1.9)$$

where K1 and K2 are the constants of the two torques.

For the reaction that represents transformation equilibrium, the potential can be written as a function of the redox potential of the two redox couples

$$\varepsilon = \varepsilon_1^0 + \frac{0,059}{z}\log\frac{[Ox_1]}{[Red_1]} = \varepsilon_2^0 + \frac{0,059}{z}\log\frac{[Ox_2]}{[Red_2]} \quad (1.10)$$

From the last equality, making the difference $\varepsilon_2^0 - \varepsilon_1^0$ on obtain:

$$\varepsilon_2^0 - \varepsilon_1^0 = \frac{0,059}{z}\log\frac{[Ox_1][Red_2]}{[Red_1][Ox_2]} = 0,059\log K \quad (1.11)$$

The mentioned considerations are important for the substrate of interest, p-nitrophenol O2N-Ar-OH, because it participates in the global reduction reaction with sodium borohydride (1.12) both in a proton exchange reaction (1.13) and in a reagent with electron exchange (1.14):

$$NaBH_4 + 2H_2O \rightleftharpoons 3H_2 + NaBO_2 \quad (1.12)$$

$$O_2N\text{-}Ar\text{-}OH + OH^- \rightleftharpoons O_2N\text{-}Ar\text{-}O^- + H_2O \quad (1.13)$$

$O_2N\text{-}Ar\text{-}O^- + 2H_2 \rightleftharpoons H_2N\text{-}Ar\text{-}O^- + 2H_2O$ (1.14)

The reduction of p-nitrophenol becomes a marker of catalytic reduction reactions, because the transformation of p-nitrophenolate into p-aminophenol can be excellently followed spectrophotometrically, equation (1.15):

The reduction of p-nitrophenol becomes a marker of catalytic reduction reactions, because the transformation of p-nitrophenolate into p-aminophenol can be excellently followed spectrophotometrically equation (1.15):

$O_2N\text{-}Ar\text{-}O^- + 2H_2 \rightleftharpoons H_2N\text{-}Ar\text{-}O\text{-} + 2H_2O$ (1.15)

$\lambda = 404nm$ $\lambda = 317nm$

At the same time, the reduction of p-nitrophenol, a very toxic substance with moderate applications as an aromatic intermediate, leads to a substance of great value in the preparation of pharmaceutical substances or dyes.

Of course, the reduction of nitroderivatives can be achieved in several ways (Figure 1.3) [7]:

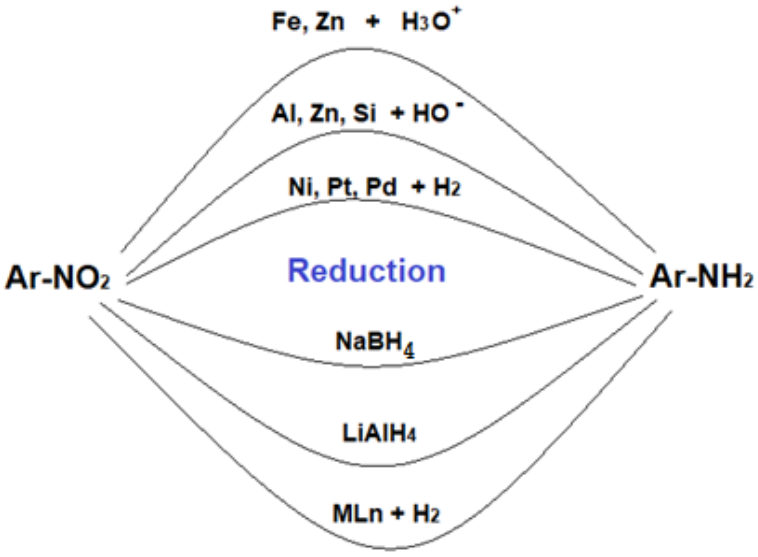

Figure 1.3. Schematic presentation of the aromatic nitro compounds reduction [7]

Because it can be carried out in an environmentally friendly environment (water), the reaction with sodium borohydride is of great importance, and because it takes place in the presence of catalysts, it can be a means of assessing their activity and efficiency.

1.4. Conclusions

Among known pollutants, those that cause significant discomfort are those that have a bad smell.

Bad-smelling pollutants are generally also very toxic.

p-nitrophenol belongs to the classes of pollutants with the above characteristics.

Incineration in power plants or through co-incineration in the cement industry leads to unwanted nitrogen oxides.

A recommended procedure for p-nitrophenol is reduction to p-aminophenol.

Catalytic hydrogenation is studied among the reduction processes in this thesis.

For the valorization of p-aminophenol, membrane separation leads to recuperative separation.

The catalytic reduction with molecular hydrogen (NaBH4 in aqueous medium) is intensively studied and the reaction mechanisms are very diverse.

The catalysts used in the reduction of p-nitrophenol are metallic, oxide or composite nanospecies.

Part B. Experimental original data

Chapter 3.

Emulsion Liquid Membranes Based on Os–NP/n–decanol or n–dodecanol Nanodispersions for p–Nitrophenol Reduction

Abstract: Membrane materials with osmium nanoparticles have been recently reported for bulk membranes and supported composite membranes systems. In the present chapter, a catalytic material based on osmium dispersed in n–decanol (nD) or n–dodecanol (nDD) is presented, which also works as an emulsion membrane. The hydrogenation of p–nitrophenol (PNP) is carried out in a reaction and separation column in which the acid receiving phase emulsion is dispersed in the osmium nanodispersion, in n–alcohols. The variables of the PNP conversion process and p–aminophenol (PAP) transport are: the nature of the membrane alcohol, the flow regime, the pH difference between the source and receiving phases and the

number of operating cycles. The conversion results are in all cases better for nD than nDD. The counter-current flow regime is superior to the co-current flow. Increasing the pH difference between the source and receiving phases amplifies the process. The number of operating cycles is limited to five, after which regeneration of the membrane dispersion is required. The apparent catalytic rate constant (k_{app}) of the new catalytic material based on the emulsion membrane with nanodispersion of osmium nanoparticles (0.1×10^{-3} s^{-1} for n–dodecanol and 0.9×10^{-3} s^{-1} for n–decanol) is lower by an order of magnitude compared to those based on adsorption on catalysts from platinum metal group. The advantage of the tested membrane catalytic material is that it extracts p–aminophenol in the acid receiving phase.

Keywords: osmium; osmium nanoparticle; osmium reduction; p–nitrophenol reduction; nanodispersion; liquid membranes; emulsion liquid membranes; undecylenic acid; n–dodecanol; n–decanol.

Rezumat: Materialele membranare cu nanoparticule de osmiu au fost raportate recent pentru membrane în vrac și sisteme de membrane compozite suportate. În capitolul de față este prezentat un material catalitic pe bază de osmiu dispersat în n-decanol (nD) sau n-dodecanol (nDD), care funcționează și ca membrană de emulsie. Hidrogenarea p–nitrofenolului (PNP) se realizează într-o coloană de reacție și separare în care emulsia de fază primitoare de acid este dispersată în nanodispersia de osmiu, în n–alcooli. Variabilele procesului de conversie a PNP și ale transportului p–aminofenolului (PAP) sunt: natura alcoolului membranar, regimul de curgere, diferența de pH dintre fazele sursă și receptoare și numărul de cicluri de operare. Rezultatele conversiei sunt în toate cazurile mai bune pentru nD decât pentru nDD. Regimul de

curgere în contracurent este superior debitului în cocurent. Creșterea diferenței de pH între fazele sursă și recepție amplifică procesul. Numărul de cicluri de operare este limitat la cinci, după care este necesară regenerarea dispersiei membranei. Constanta aparentă a vitezei catalitice (kapp) a noului material catalitic bazat pe membrana de emulsie cu nanodispersie de nanoparticule de osmiu (0,1 × 10−3 s−1 pentru n-dodecanol și 0,9 × 10−3 s−1 pentru n-decanol) este mai mică cu un ordin de mărime în comparație cu cele bazate pe adsorbția pe catalizatori din grupa metalului platină. Avantajul materialului catalitic membranar testat este că extrage p-aminofenolul în faza de primire a acidului.

Cuvinte cheie: osmiu; nanoparticule de osmiu; reducerea osmiului; reducerea p-nitrofenolului; nanodispersie; membrane lichide; membrane lichide de emulsie; acid undecilenic; n-dodecanol; n-decanol.

3.1. Introduction

Liquid membranes are systems made up of three immiscible phases: an aqueous source phase, which contains the chemical species of interest for valorization or removal from the system, an organic membrane phase that ensures the selective transport of the considered chemical species and an aqueous receiving phase in which it will be immobilized [1–3]. Liquid membranes are usually differentiated based on the amount and form in which the membrane phase is found in the system, in: volume liquid membranes (bulk liquid membranes, BLM), liquid membranes on support (supported liquid membranes, SLM) and emulsion liquid membrane (emulsion liquid membranes, ELM) [4–6]. The liquid membranes have been continuously developed because they ensure transport selectivity, allow chemical reactions in the source, membrane and receiving phases, and can be made in various designs in order to meet process requirements (low investments, productivity, large contact surfaces, easy operation) [7–10]. From the scale-up point of view, SLM and ELM (Figures 3.1a and 3.1b) are

in direct competition in order to optimize: the contact surface between the phases, the stability of the membrane and the losses of membrane material in the aqueous phases, the recovery of the solvent membrane and of the chemical species of interest [11–13]. Liquid membranes, usually those based on organic solvent, consist of a pure solvent, a solution or a dispersion in which the continuous phase is the membrane solvent [14,15]. The chemical species that are added to the membrane solvent mainly have the role of transporter [16], but more and more often they also ensure the catalysis of a reaction process that takes place in the membrane to favor the separation in the desired chemical form of the target chemical species (Figure 3.1c) [17].

In this chapter, the target chemical species is p–nitrophenol, both because it can be easily reduced with molecular hydrogen, and because this reaction can be observed through accessible means (UV-Vis, from yellow to colorless) [18].

The reactive membrane systems recently tested for the reduction and separation of p–nitrophenol (pNP) from source aqueous solutions, use polymers as membrane phases (Figure 3.1d) or medium-chain n–alcohols, in which nanoparticles are dispersed [19–23].

The source of metallic osmium is represented by the remains (waste) of osmium tetroxide (OsO_4) recovered in a polar or non-polar solvent, which makes it usable in reactions a homogenous medium, which aim to obtain osmium nanoparticles, through reduction [19,20].

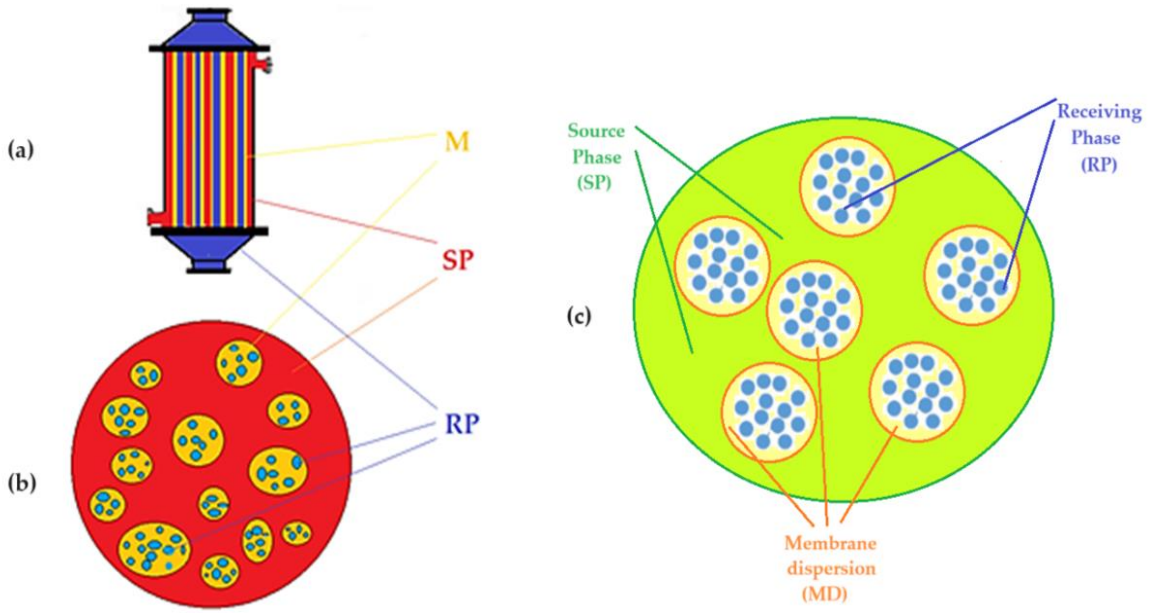

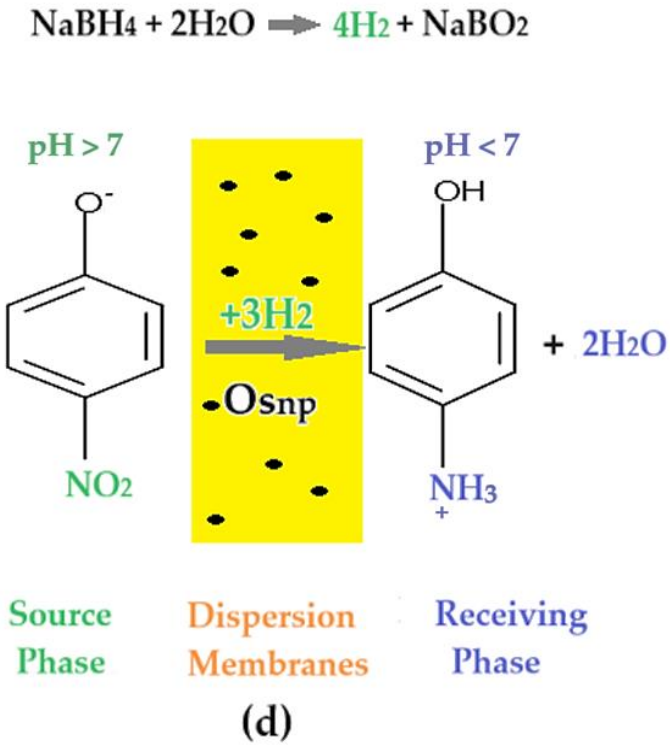

Figure 3.1. (a) Supported liquid membrane (SLM); **(b)** emulsion liquid membrane (ELM); **(c)** proposal reactional membrane systems; **(d)** catalytic p–nitrophenol reduction with molecular hydrogen through osmium–nanoparticles membrane [19,20,30,31]; M: membrane (Os–NP/n–alcohol dispersion; SP: source phase (p–nitrophenol + sodium tetrahydride in alkaline aqueous solution); RP: receiving phase (acid aqueous solution).

The osmium recovery process involves fixing or removing oxygen from osmium tetroxide (equation (1)):

$$OsO_4 + Red \rightarrow Os + Ox \qquad (3.1)$$

Of course, it is preferable that the reductant or its reaction products are not necessarily removed from the reaction mass [22–26].

The osmium nanoparticles obtained in this way were used both in oxidation and reduction processes with membrane systems [19,20], but the proposed membrane systems did not have the expected impact among researchers. The reluctance that researchers have regarding the use of osmium as catalyst refers in particular to its toxicity, related to the increased volatility of osmium tetroxide, but also to the aggressiveness of this oxide on the human body, since tetroxide seems to react with the side chains of the proteins [27–29]. Thus, because of the concerns regarding the toxicity of osmium, but mainly due to the apparent reaction rate constant

close to, but lower than most nano-metric catalysts, based on platinum metals, it was less often used [19,20,30,31].

The emulsion membrane type system proposed in this paper (Figures 3.1b and 3.1c) is based on the reaction system from Figure 1d. The choice of the system with emulsion membrane is clearly different from the recently studied reaction systems [19,20,30,31]. Emulsion membranes ensure a large contact surface, a micrometric membrane film for mass transfer and chemical reaction [32–38], the possibility of choosing some green solvents as membranes (saturated n–alcohols).

The study of osmium nanodispersion in n–dodecanol as membrane phase compared to n–decanol [30] is argued by the lower volatility of n–dodecanol, which contributes to the reduction of membrane phase losses in aqueous phases and atmosphere. At the same time, the precaution related to maintaining the working temperature is wider compared to n–decanol. The operating time in the emulsion membrane system is much lower than in bulk liquid membrane and supported liquid membrane systems.

On the other hand, the osmium nanoparticles were synthesized by various procedures, depending on their destination [39–42].

In this chapter we study nanodispersions with osmium nanoparticles obtained by synthesis from osmium tetroxide reduced with undecenoic acid in n–dodecanol (nDD) or n–decanol (nD) medium. The catalytic activity was determined by the reduction of p–nitrophenol (pNP) to p–aminophenol (pAP) in an emulsion membrane system. In this case, the membrane in the emulsion membrane system is the osmium nanodispersion in the chosen organic solvent, the source phase is an aqueous solution of p–nitrophenol and sodium tetraborate, and the receiving phase is an acidic aqueous solution. The operation of the proposed system takes place both in co-current and counter-current, the pH gradient being a working variable.

3.2. Results

The obtained results in this work were systematized in:

- ✓ Morphological characterization of nanodispersions in n–dodecanol by transmission electron microscopy (TEM), scanning electron microscopy (SEM) and dynamic light scattering (DLS);
- ✓ Compositional characterization of nanodispersions in n–dodecanol performed by energy-dispersive spectroscopy analysis (EDAX) and thermal analysis coupled with gas chromatography (GC) and Fourier Transform InfraRed spectroscopy (TA–GC–FTIR);

- ✓ Determination of the process performances of nanodispersions of osmium particles in n–decanol or n–dodecanol for the reduction of p–nitrophenol.

In this chapter, the characterization data for n–decanol have not been emphasized except where strictly necessary, because they were recently reported by the co-authors [30].

3.2.1. Morphological characterization of the obtained nanodispersions

The TEM characterization of osmium nanodispersions in n–dodecanol was performed by washing with ethanol, which would have assumed the possibility of visualizing individual osmium nanoparticles. Unexpectedly, in the obtained images (Figure 3.2), the sample has an alveolar appearance with walls containing osmium nanoparticles. We can state that, despite the sample preparation (washing) with ethanol, the osmium nanoparticles remain covered by the organic solvent. Thus, the observed aggregates separate in the alveolar walls containing n–dodecanol, both before the p–nitrophenol reduction process (Figure 3.2a) and after processing (Figure 3.2b). Unfortunately, this organic coating prevented the increase in the resolution of the images, because the sample shows an internal combustion of the alcohol with the osmium nanoparticles, which is practically highlighted by the disappearance of matter in the examined areas. The affected areas present themselves as bright spots, confirming an observation previously described in the literature [30].

Although they were difficult to obtain, the images allow the observation of aggregates of osmium nanoparticles as well as individual particles of about 10–50 nm.

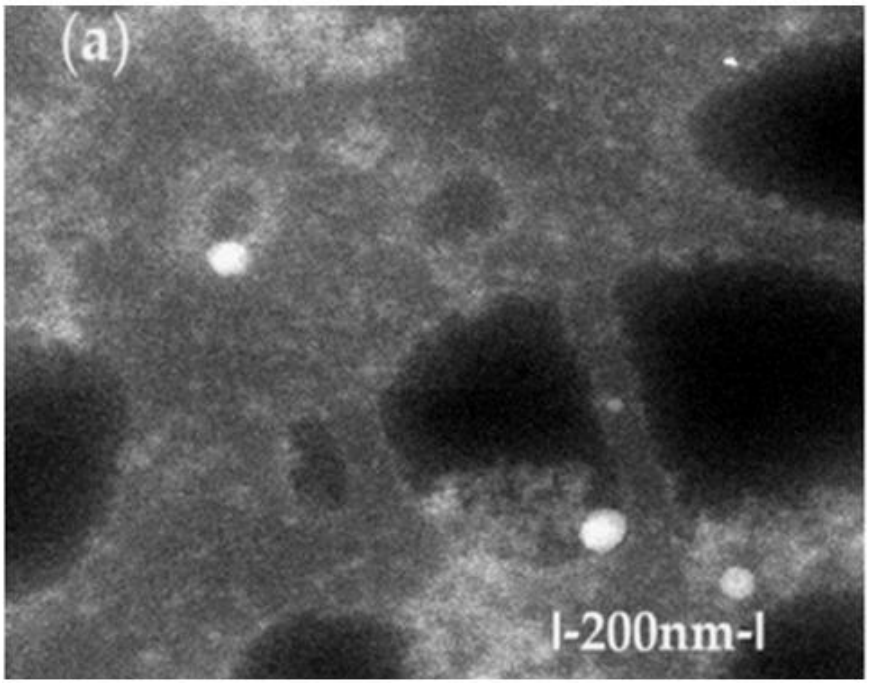

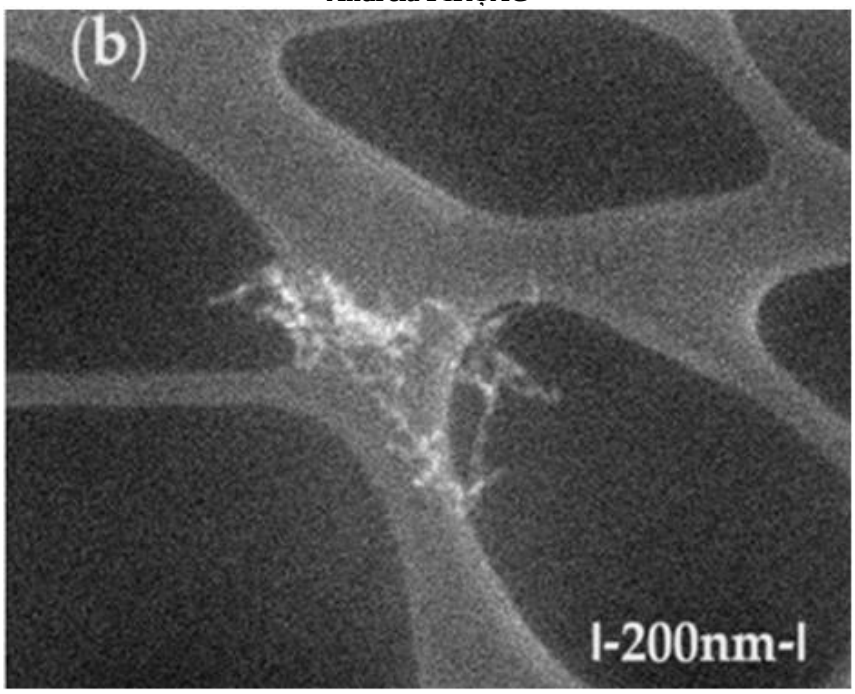

Figure 3.2. The scanning electronic microscopy (SEM) images for Os/ n–dodecanol nanodispersions **(a)** before use; and: **(b)** after use; in the reduction process of p–nitrophenol.

In order to avoid the oxidation observed in the transmission electron microscopy (TEM) analysis, scanning electronic microscopy (SEM) examination was attempted. Thus, the dispersion deposited on an aluminum support was dried in vacuum and covered with a 50 nm gold film. Through this process, overheating of the sample was avoided, obtaining the morphology of the aggregates from the primary nanodispersion of osmium/ n–dodecanol (Figure 3.3a) and those obtained after the p–nitrophenol reduction process (Figure 3.3b). After processing in the p–nitrophenol reduction process, the morphology of the dispersions does not change drastically (Figure 3.3b), but the aggregates of osmium nanoparticles are more easily visible.

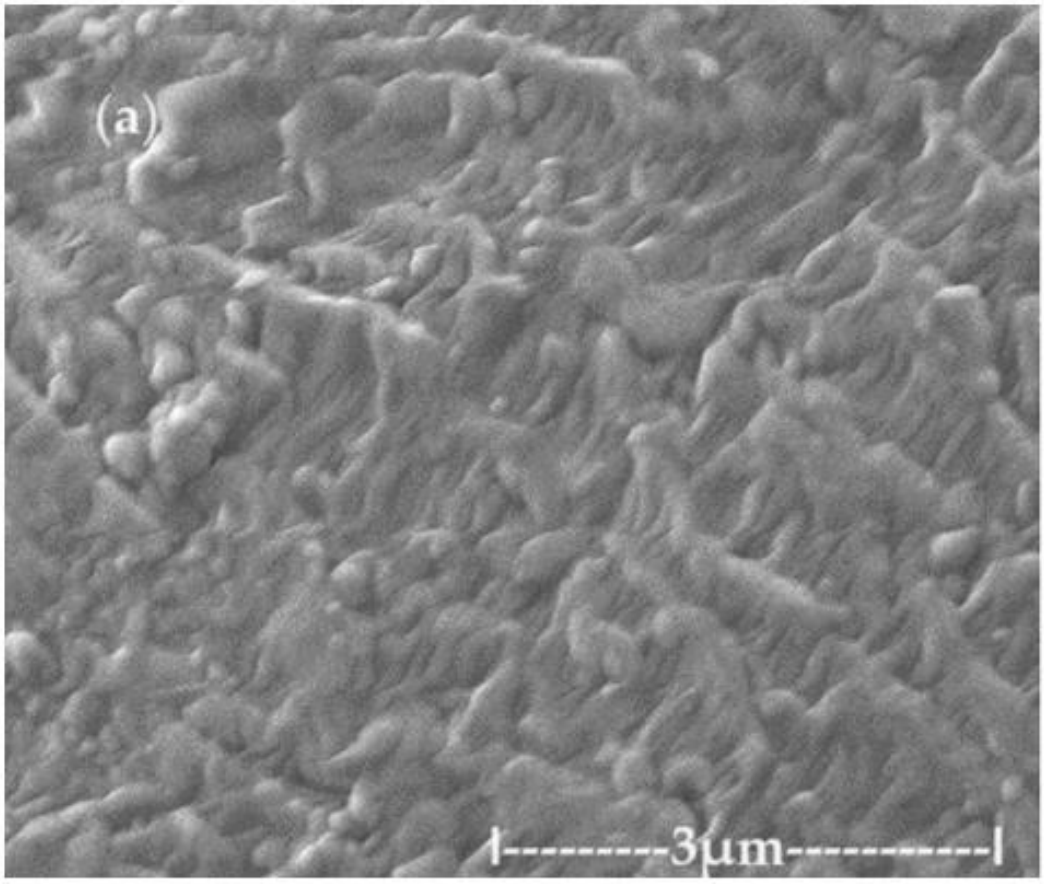
(a)
|--------3μm----------|

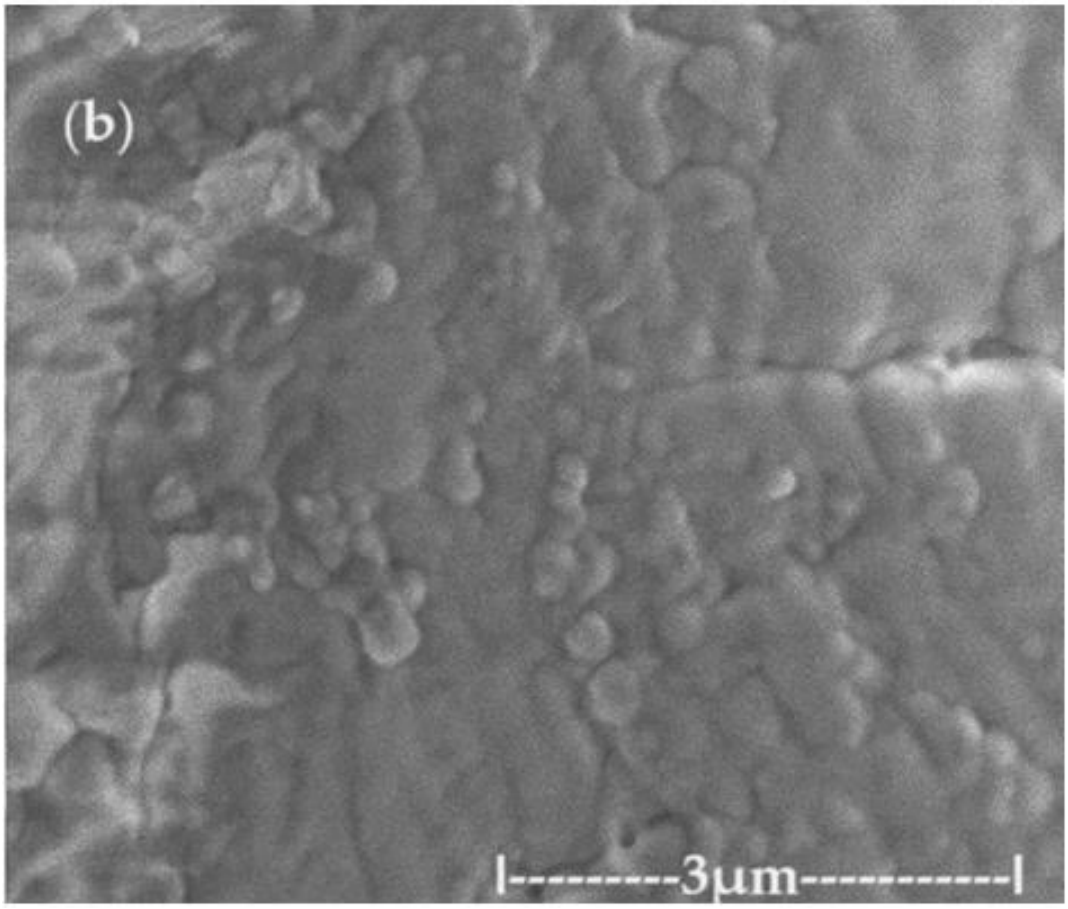
(b)
|--------3μm----------|

Figure 3.3. The images obtained by scanning electronic microscopy (SEM): for the primary Os/n–decanol dispersion **(a)**; and for the Os/n–dodecanol dispersion **(b)**; obtained after the p–nitrophenol reduction process.

In order to obtain the size of osmium nanoparticles and their aggregates, dynamic light scattering (DLS) analysis was performed, after dispersing the sample in isopropyl alcohol.

Dynamic light scattering (DLS) analysis shows two-peak curves of some Gaussian-type distributions (Figure 3.4).

The analysis of the dimensional distribution of the nanodispersion before use in the reduction process of p–nitrophenol (Figure 4a) does not essentially differ from the dimensional distribution of nanodispersion after the reduction process (Figure 4b). At the nanodispersion in isopropanol, two Gaussian distributions between 4 nm and 70 nm and between 200 nm and 1200 nm can be observed initially (Figure 4a). In the case of the second dispersion in isopropanol (Figure 4b) the Gaussian distribution widens at small sizes (from 4 nm to 170 nm) but narrows at large sizes (300 nm to 1000 nm).

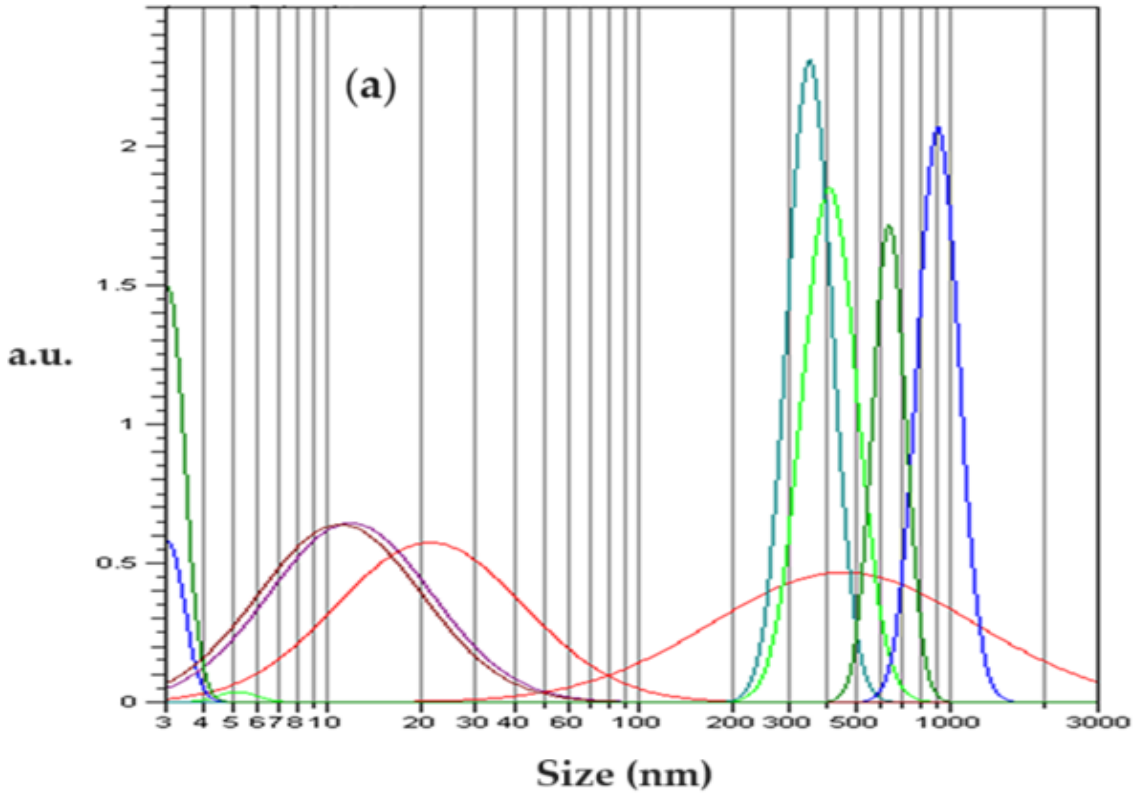

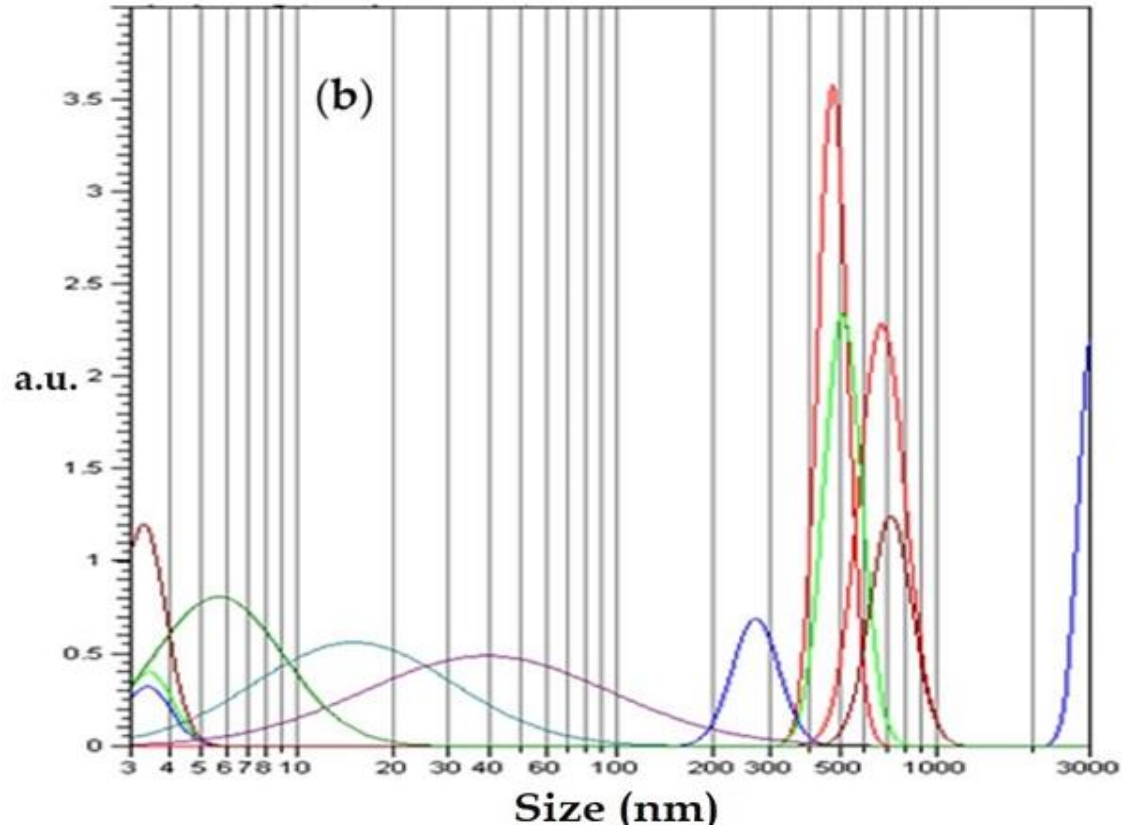

Figure 4. Size distribution of osmium nanoparticles in dispersion in isopropanol: **(a)** before use; and: **(b)** after use; in the p–nitrophenol reduction process.

The dimensional analysis of nanodispersions of osmium nanoparticles in n–dodecanol provides the following information:

- ✓ Transmission electron microscopy (TEM) reveals agglomerations of nanoparticles from 10 nm to 30 nm both before and after the processing of the nanodispersions in the reduction process of p–nitrophenol;
- ✓ Scanning electron microscopy (SEM) image analysis confirms the nanoparticle sizes in the nanodispersion;
- ✓ Dynamic light scattering (DLS) analysis most relevantly indicates the size of nanoparticles in the range of 5 nm to 20 nm, as well as aggregates of nanoparticles with dimensions of 0.3 μm to 1.1 μm.

3.2.2. Compositional characterization of the obtained nanodispersions

The composition of the dispersion of osmium nanoparticles had the following objectives:

- ✓ Determination of the composition and distribution of nanoparticles in nanodispersion by energy-dispersive spectroscopy analysis (EDAX).

- ✓ Determination of the composition of the solvents that remain in the nanodispersion after repeated washing with water by thermal analysis coupled with gas chromatography and Fourier transform infrared spectroscopy (TA–GC–FTIR).

Figure 3.5 shows the spectrum of the nanodispersion in which the carbon atoms generated by organic solvents and elemental osmium are present. The distribution map of the two elements is uniform in nanodispersion, which ensures its stability.

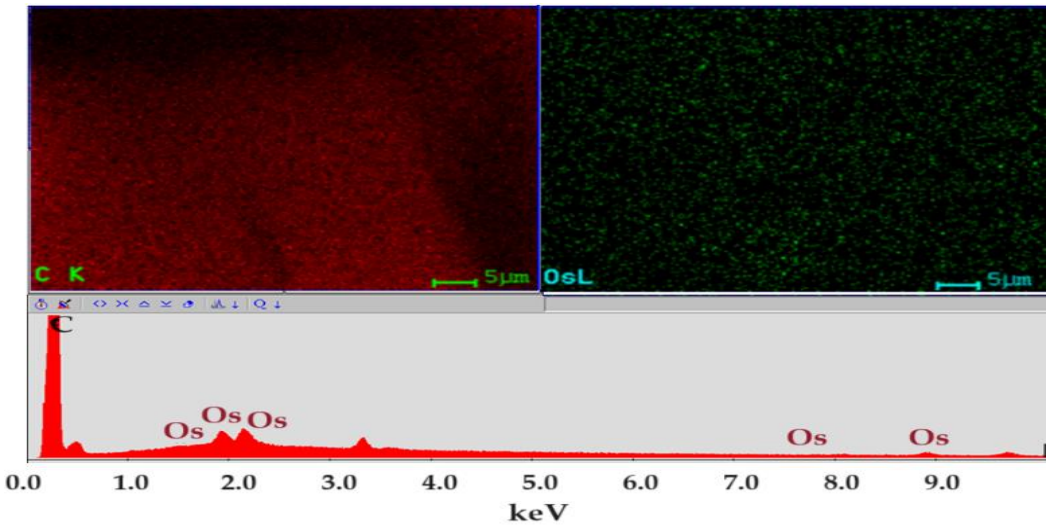

Figure 3.5. Energy-dispersive spectroscopy analysis (EDAX) for osmium nanodispersion in n–dodecanol.

Thermal analysis (TG and DSC) was performed to determine the composition of the solvents in nanodispersion. The analyses were carried out in an N_2 atmosphere, so no oxidation of the organic substance or osmium is foreseen.

Os/n–dodecanol (nDD) dispersion in comparison with n–decanol (nD) dispersion sample (Figure 3.6a, Table 3.1) is starting to lose the liquid part over 125 °C, the evaporation between 125–220 °C representing 89.87% of the initial mass. The process is accompanied, on DSC curve, by an endothermic effect with the minimum at 196.1 °C, generated by the evaporation of the solvent, undecylenic acid, but the boiling point is lower than the value reported by literature, i.e. 275 °C. The residual mass is 4.46% and is consisting of osmium compounds (Figure 3.6b).

In the two-dimensional and three-dimensional FTIR spectra for Os–nDD up to 200°C (Figures 3.6c and 3.6d), the presence of CO_2 is mostly seen at 2355 cm^{-1}, traces of CO at 2169cm^{-1}, water, but also the corresponding vibration of Csp^3–H at 2964 cm^{-1}. A small peak is observed at 3072 cm^{-1} corresponding to Csp^2–H fragments (Figures 3.6c and 3.6d) [31].

As the temperature increases, the peak from 1721 cm^{-1} is attributed to C=O bond from undecylenic acid, which is eliminated at higher temperatures (Figure 3.6c) and is not completely consumed when preparing the dispersion by reduction [20,30,31].

Table 3.1.

The thermal characteristics of the dispersion diagrams of osmium nanoparticles in n–decanol and n–dodecanol.

Sample	**Mass loss up to**	**Solvent removal**	**Endo peak**	**Residual mass**
n–decanol	1.96% at 95 °C	94.94% between 95–220 °C	156.8 °C	1.70%
n–dodecanol	1.46% at 125 °C	89.87% between 125–220 °C	196.1 °C	4.46%

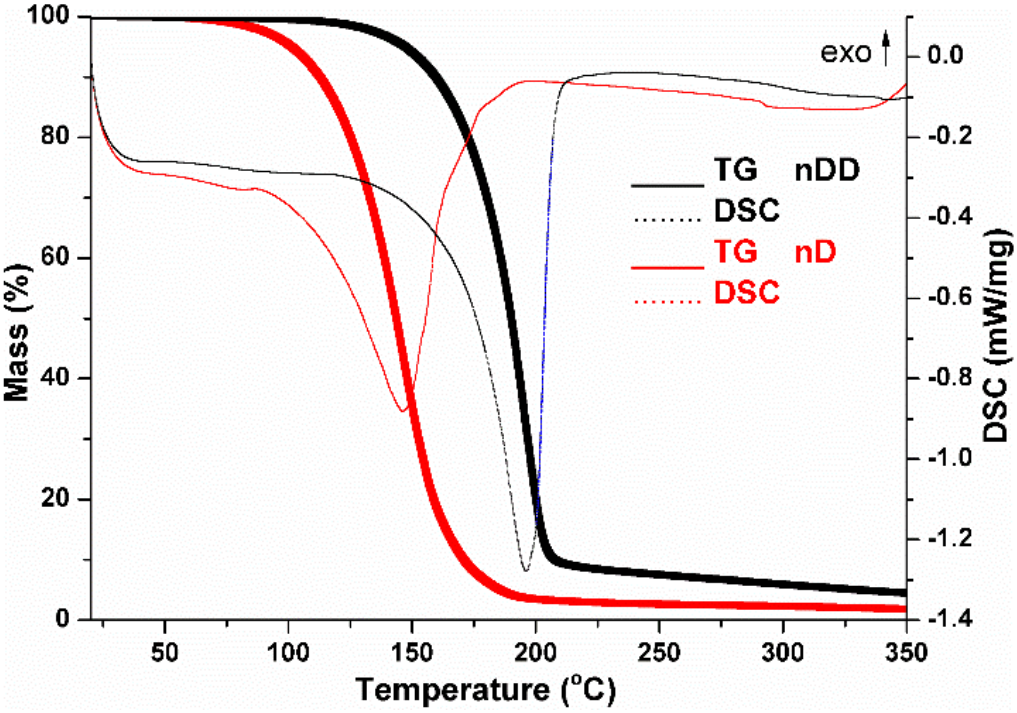
exo
TG nDD
DSC
TG nD
DSC
Mass (%)
DSC (mW/mg)
Temperature (°C)

(a)

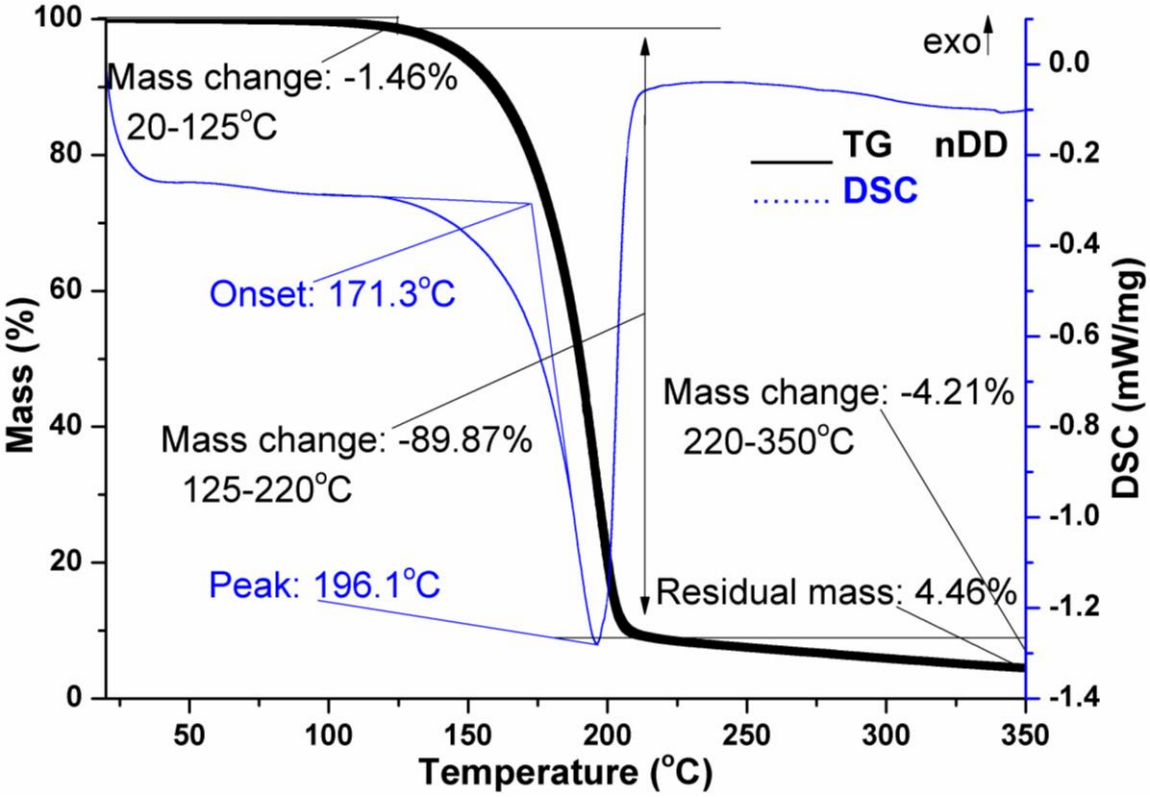
Mass change: -1.46%
20-125°C
Onset: 171.3°C
Mass change: -89.87%
125-220°C
Peak: 196.1°C
Mass change: -4.21%
220-350°C
Residual mass: 4.46%
exo
TG nDD
DSC
Mass (%)
DSC (mW/mg)
Temperature (°C)

(b)

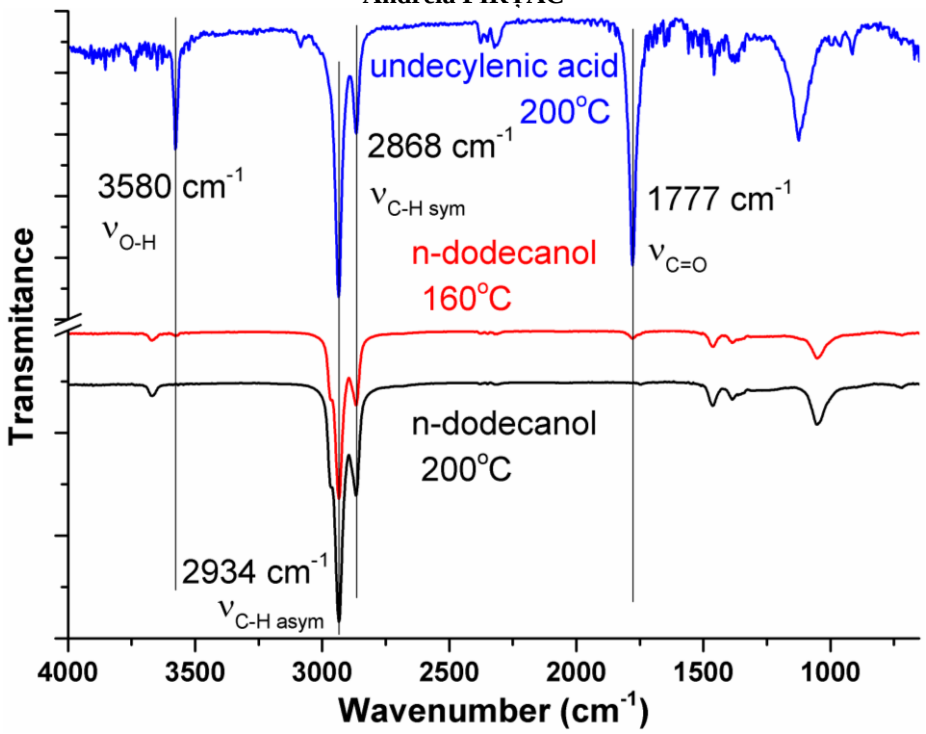

(c)

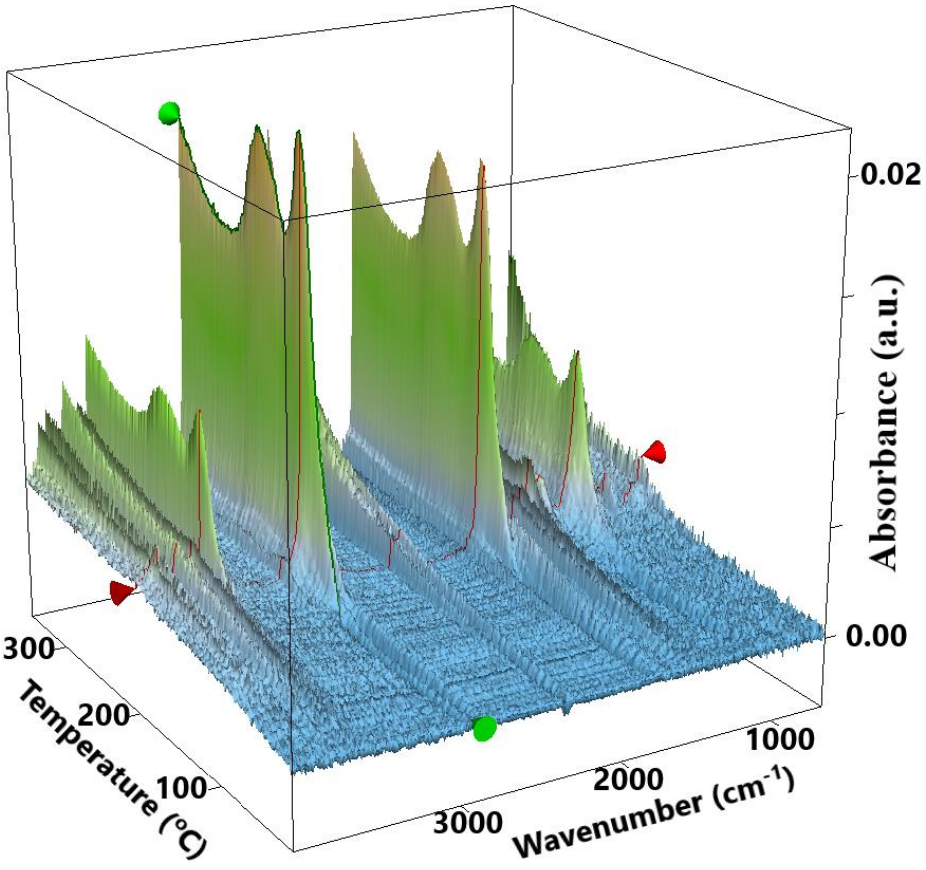

(d)

Figure 3.6. Thermal analysis **(a)** and **(b)**; and FTIR analysis of decomposition gases: two-dimensional FTIR **(c)**; and three-dimensional FTIR **(d)**.

The compositional characterization of osmium nanoparticle nanodispersions in n–alcohols show that:

- ✓ Osmium nanodispersions in n–dodecanol have the elemental composition (EDAX) which indicates the presence of carbon and osmium;
- ✓ The distribution map (EDAX) of the two elements, osmium and carbon, shows uniformity on the surface;
- ✓ The thermal analysis coupled with gas chromatography and Fourier Transform InfraRed (TA–GC–FTIR) of the n–dodecanol based nanodispersion highlights the presence of n–decanol, but also of unreacted undecylenic acid.

3.2.3. Determining the process performances for p–nitrophenol reduction

The chosen chemical species for conducting the experiments is p–nitrophenol, for which the specialized literature provides numerous and conclusive data [19,20,30,31]. At the same time, p–nitrophenol is a toxic substance that is easy to follow spectrophotometrically, when it passes, through reduction, in p–aminophenol [20,30–39]. In this paper, the accuracy of the determinations is ±0.3%, imposed both by the method of sampling and preparation of the samples, as well as by the interaction of the chemical species dissolved in the aqueous phase with nitrophenol (alkaline medium, sodium ions, n–alcohols).

The experiments show the results of p–nitrophenol reduction to p–aminophenol using an ELM, which contains the acidic aqueous receiving phase (blue) found inside the nanodispersion emulsion containing osmium nanoparticles (yellow), and an aqueous basic source phase (green) containing p–nitrophenol and sodium borohydride, outside the emulsion (Figure 6.1).

In our case, the temperature at which the studies were carried out was 24 ± 1 °C.

Although, according to Arrhenius equation, the studies had to include the operating temperature variation, this was not done for two reasons:

- ✓ Increasing the temperature favors the volatility of alcohols and therefore, losses of membrane solvent.
- ✓ The stability of emulsion membrane decreases with the increasing temperature.

Temperatures lower than that of the laboratory were not taken into account both from the point of view of technical complications and the increase in the viscosity of alcohols, thus the decrease in mass transfer.

The reduction reaction takes place in a column-type reactor fed at the base with emulsion containing the receiving phase, and the source phase is introduced either at the base of the column (co-current) (Figure 3.7a) or at the top (counter-current) (Figure 3.7b).

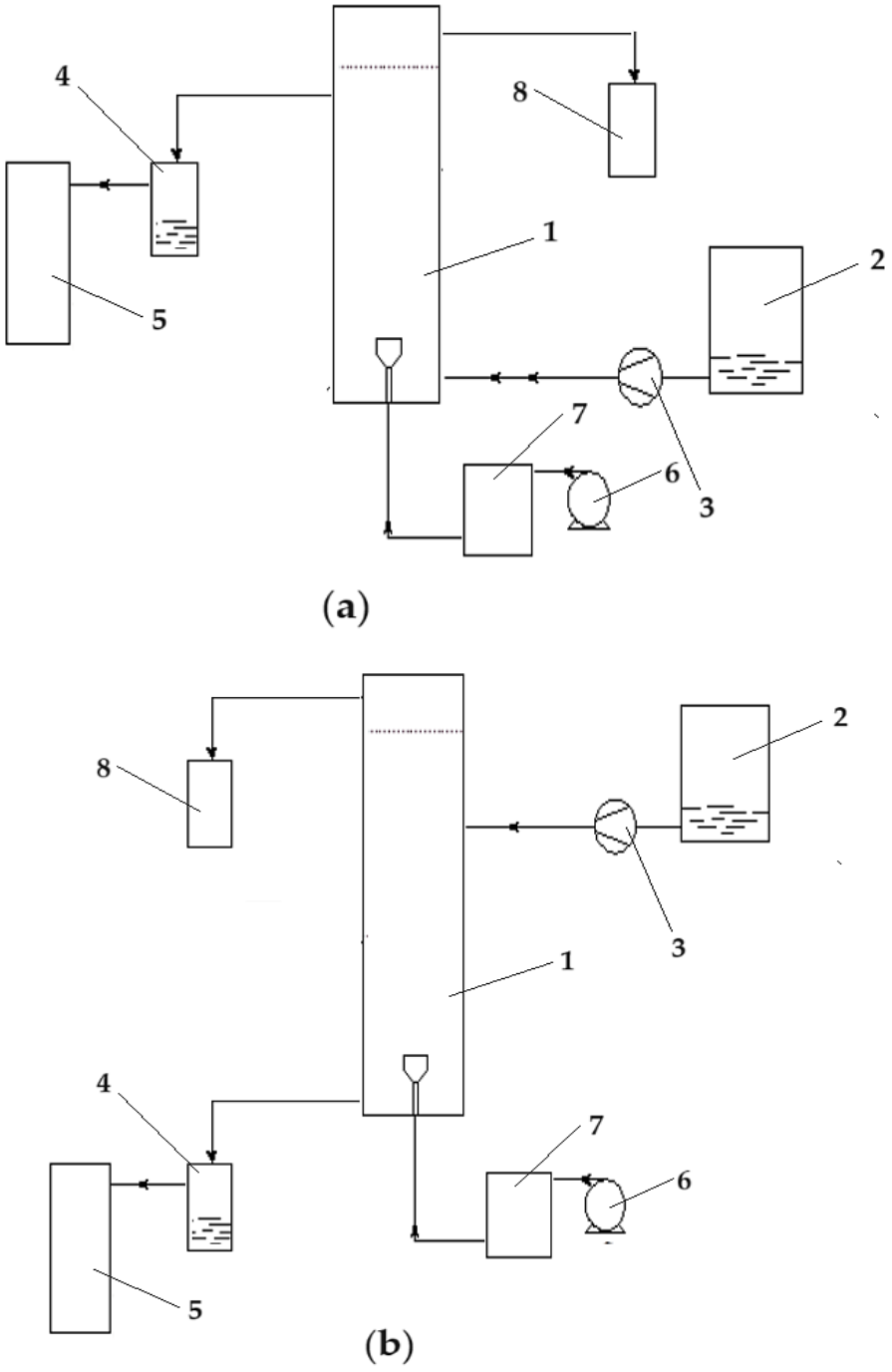

Figure 3.7. Phase circulation in the column for the reduction of p–nitrophenol to p–aminophenol: **(a)** co-current; and **(b)** counter-current. 1 – the reaction column; 2 – source phase (SP) tank; 3 – source phase metering pump; 4 – source phase level maintenance vessel; 5 – source phase tank; 6 – emulsion dosing pump; 7 – intermediate emulsion vessel; 8 – emulsion collector vessel.

The conversion (η %) or extraction efficiency (*EE*%) for the species of interest using the concentration of the solutions [19–21] was calculated as follows:

$$\eta\% \; or \; EE(\%) = \frac{(c_0 - c_f)}{c_0} \cdot 100 \tag{3.2}$$

where: c_f is the final concentration of the solute (considered chemical species) and c_0 is the initial concentration of solute (considered chemical species).

The same extraction efficiency can also be computed based upon the absorbance of the solutions [30,31], as in:

$$\eta\% \; or \; EE(\%) = \frac{(A_0 - A_s)}{A_0} \cdot 100 \tag{3.3}$$

where: A_0 is the initial absorbance of sample solution and A_s is the current absorbance of the sample.

At a pH higher than 10 of the source phase and a pH less than 4 of the receiving phase, the results of conversion (η) of p–nitrophenol to p–aminophenol, with the emulsion based on alcoholic nanodispersion containing osmium nanoparticles, are superior to those presented previously [20,30,31], using supported liquid membranes (SLM) or bulk liquid membranes (BLM). This observation determined the study of the conversion of p–nitrophenol with emulsion membranes based on osmium nanoparticles and n–decanol or n–dodecanol.

The current data are presented by comparing the results obtained with the nanodispersion of n–dodecanol (curve with brown squares) and, respectively, in n–decanol (curve with green triangles) (Figure 3.8), in a co-current system. Throughout the process, the conversion obtained with the nanodispersion based on n–decanol is superior to that based on n–dodecanol, in the average operating range of 6–18 minutes. The flattening of the conversion value after 20 minutes of operation is related to the exhaustion of working reagents.

In the stripping column with emulsion membranes containing drops of the aqueous phase of pH 2 and source aqueous solution of pH 12, the conversion (η) was studied depending on the type of the membrane solvent and on the flow mode of the phases. Over the entire the working range, the conversion results obtained with membranes based on n–decanol (green triangles and black crosses) are superior to those obtained with dispersion in n–dodecanol (blue diamonds and brown squares) (Figure 3.9).

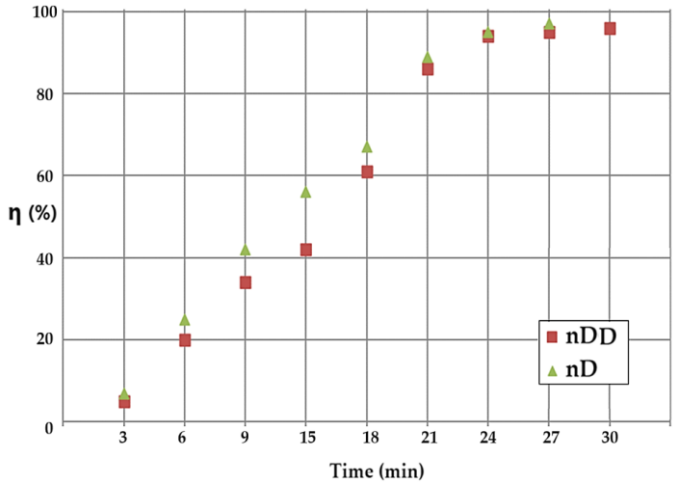

Figure 3.8. Comparison of the results, as a function of time, obtained from the conversion of p–nitrophenol with the nanodispersion of n–dodecanol (brown squares), and respectively, n–decanol (green triangles), in counter-current operating system.

At the same time, the results of the conversion obtained in the counter-current flow version (brown squares and black crosses) are superior to those obtained by the recirculation of the phase in co-current (blue diamonds and green triangles) (Figure 3.9).

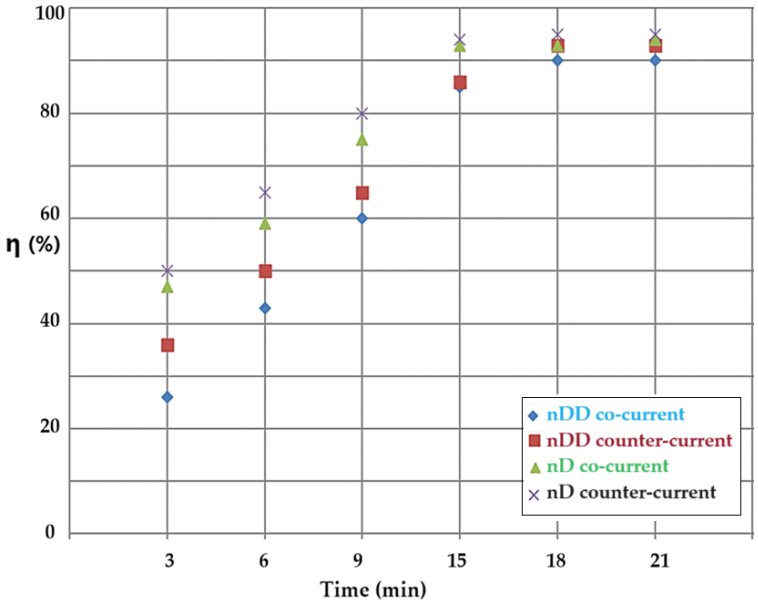

Figure 3.9. Comparison of the results obtained during the conversion (η) of p–nitrophenol with the nanodispersion of n–dodecanol (blue diamond, brown squares), and respectively, of n–decanol (green triangle and black crosses) depending on time and the flow mode of the phases in the stripping column: counter-current (brown square and black crosses) and co-current (blue diamonds and green triangles).

The operation of the counter-current reaction system ensures a relatively equal concentration gradient of the reactants during the reaction and mass transfer, while in the case of co-current operation the concentration gradient decreases constantly [42]. After approx. 15 minutes of operation, when the concentration difference of the reactants is minimal, the capping effect of the conversion appears. Basically, when high conversion is desired, countercurrent operation is preferable when the working time is minimized. If the operating time is not an impediment to the reaction and mass transfer process, then either type of flow can be chosen.

By choosing the experimental variant with the circulation of the aqueous phase, the basic source in counter-current with the nanodispersion based on n–decanol or n–dodecanol containing drops of the acidic aqueous phase, the conversion variation (η) was followed according to the pH difference between the aqueous phases, at an operating time constant for 15 minutes. (Figure 3.10). The pH difference between the source and receiving phases is achieved with aqueous solutions of sodium hydroxide and sodium tetrahydride, respectively with hydrochloric acid and ultrapure water (Table 3.2). The pH difference is measured before processing. During the reduction of p–nitrophenol and the transport of p–aminophenol, the technical conditions, in particular the distribution of n–alcohols on the surface of the measuring electrode, cannot be monitored, neither the pH value nor its gradient.

The conversion of p–nitrophenol to p–aminophenol increases with the increase in the pH difference between the aqueous phases of the membrane system (Figure 10). Thus, if the pH difference between the source and receiving aqueous phases is 4 units then we have a conversion of 69%, and at a difference of 12 units we have a conversion is of 98% for n–decanol, and from 60% to 85%, respectively, for n–dodecanol. Practically, if we aim for an optimal conversion, then the difference in pH between the aqueous phases must be at least 9 units.

An important aspect of the study of catalytic materials is the regeneration problem. Even more so in membrane-type heterogeneous catalysis, this aspect must be treated carefully. Figure 11 shows the conversion (η) values for 5 cycles of reuse of the ELM based on osmium nanodispersions in n–decanol. The cyclic catalysis process was carried out with the emulsion based on osmium nanoparticles in n–decanol, in counter-current with the source phase of pH 12. The receiving aqueous phase, of pH 2, is recirculated as such, by means of the nanodispersion. The pH 12 source phase is refreshed at each reaction cycle with an equal concentration of p–nitrophenol and sodium borohydride.

Table 3.2. Achieving of pH difference between the source and receiving phases.

pH Receiving phase	6	5	5	4	4	3	3	2	2
pH Source phase	10	10	11	11	12	12	13	13	14
ΔpH	**4**	**5**	**6**	**7**	**8**	**9**	**10**	**11**	**12**

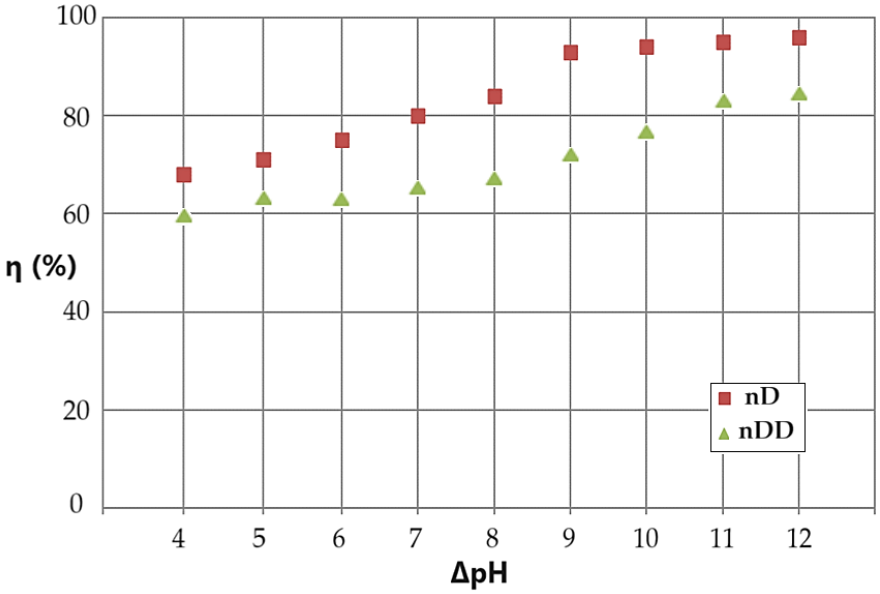

Figure 3.10. Results of the conversion (η) depending on the pH difference between the source and receiving phases, which circulate in counter-current for the emulsion based on n–decanol (brown squares) or n–dodecanol (green triangles).

The decrease in conversion by almost twenty percent depending on the number of contact cycles of the phases is caused by the increase in pH in the receiving phase, which determines a decrease in the pH differences between phases, although the pH of the source phase remains relatively constant, to the value 12. In the case of dodecanol (Figure 3.11), the initial conversion is lower (approx. 83%), but the decrease depending on the number of cycles is smaller, at approx. 78%. Practically, if the catalytic emulsion is to be reused, the one based on n–dodecanol is more advantageous, and if a higher conversion is desired, the one based on n–decanol is used, but the number of reuse cycles will be reduced.

The catalytic activity of both systems decreases because the osmium nanoparticles aggregate, thus lowering, at each operating cycle, the interphase contact surface. After five cycles of use, the decrease in catalytic activity requires regeneration of membrane nanodispersion.

The extraction efficiency (*EE*) of p–aminophenol was determined by separating the emulsion membrane in the nanodispersion containing osmium nanoparticles in n–dodecanol, and the receiving aqueous phase of pH 12. For the separation of the phases from the emulsion (collapse or breaking of the emulsion) a membrane based on cellulose acetate was used in a Sartorius ultrafiltration module of the dead-end filtration type. The results of p–aminophenol extraction efficiency is presented in Figure 3.12. It is noted that the separation efficiency starts with low values in the first-time interval, then it develops rapidly until reaching the value of 75–80%. The separation efficiency with n–decanol membranes is superior over the entire time interval to that with n–dodecanol-based membranes.

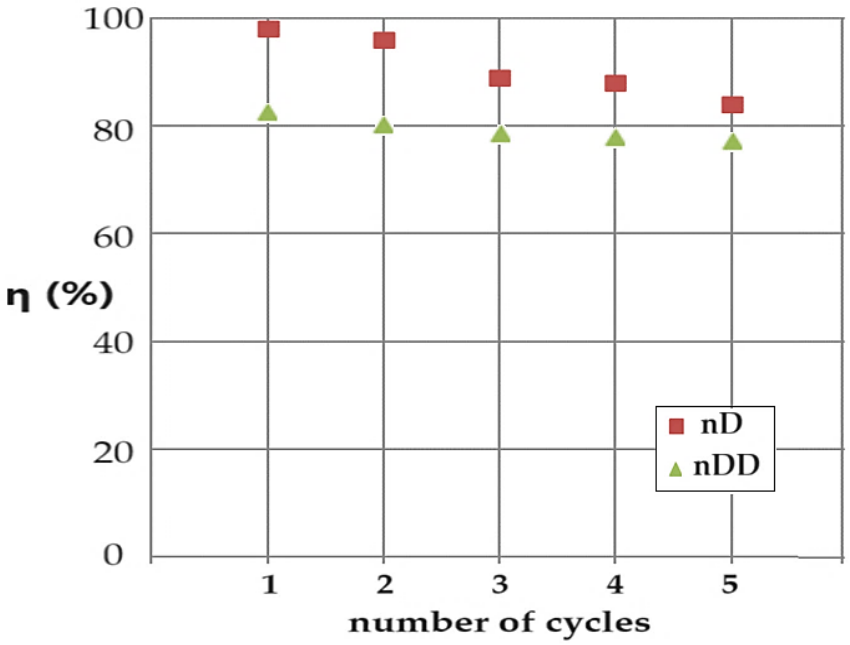

Figure 3.11. Conversion results (η) depending on the number of conversion cycles with the same emulsion based on osmium nanoparticles in n–decanol (brown squares) or n–dodecanol (green triangles), containing the receiver phase of pH 2, and the source phase of pH 12 containing p–nitrophenol and refreshed sodium borohydride, which circulates in the counter-current.

The delay in the separation of p–aminophenol compared to the conversion of p–nitrophenol to p–aminophenol can be justified both by the diffusion process through the liquid membrane and by the slow transfer from the liquid membrane to the acidic environment of the receptor phase. The extraction efficiency value is lower than the conversion value at the same operating time.

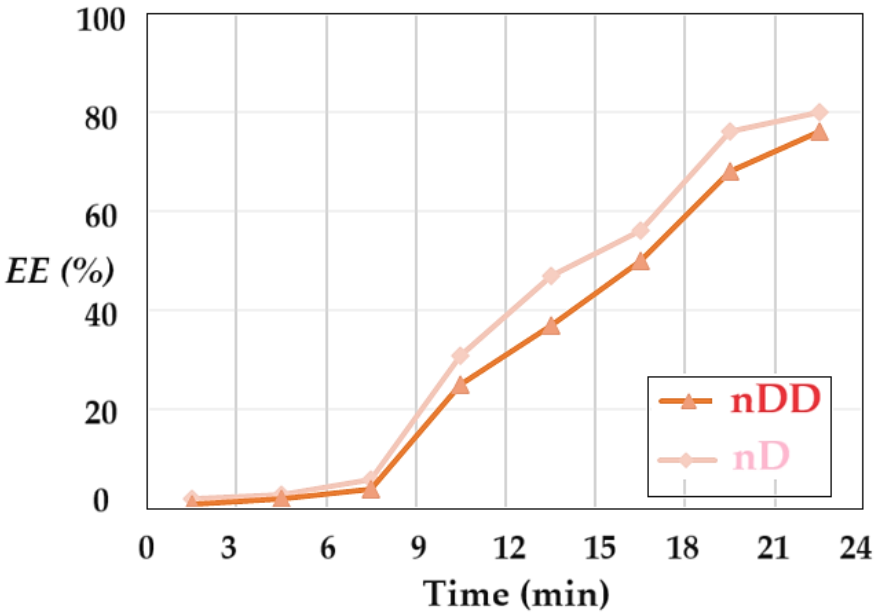

Figure 3.12. The separation efficiency (EE) of p–aminophenol from the emulsion formed by osmium nanodispersion in n–dodecanol or n–decanol and the receiving aqueous phase of pH 2, depending on the operating time.

The performances determination of the process of reducing p–nitrophenol to p–aminophenol, with osmium nanodispersions in n–decanol and n–dodecanol, in the liquid membrane emulsion system, shows that:

The liquid membrane emulsion system consists of:

The aqueous source phase of alkaline pH, containing p–nitrophenol and sodium borohydride;

1. The membrane phase – dispersion of osmium nanoparticles in n–decanol or n–dodecanol;
2. The receiving phase solution of acid pH.

- ✓ The installation (working plant) allows the co-current or counter-current circulation of the phases, the basic source and the emulsion, which contains drops of acidic aqueous solution in the osmium nanodispersion in n–decanol or n–dodecanol;
- ✓ The system that operates with nanodispersion in n–decanol ensures a conversion of p–nitrophenol to p–aminophenol, higher than nanodispersion in n–dodecanol;
- ✓ Counter-current operation of the phases leads to higher conversions than co-current operation;

- ✓ At the same operating time, the increase in the pH difference between the source and receiving aqueous phases leads to the increase in the conversion of p–nitrophenol to p–aminophenol;
- ✓ Repeating the use of the catalytic emulsion, containing osmium nanodispersions in n–alcohols, in a counter-current flow regime, decreases the conversion value from approx. 98% in the first cycle, to approx. 83% in the fifth cycle for n–decanol and from 60% to 85% for n–dodecanol;
- ✓ The p–aminophenol separation efficiency is below the p–nitrophenol conversion value over the entire operating time interval.

3.3. Discussion

Various catalytic materials for the reduction of p–nitrophenol to p–aminophenol have been recently reported and have very good results both in terms of conversion and catalyst regeneration [43–51].

In this chapter, catalytic systems comparable to the results obtained in the Os–NP/n–decanol or n–dodecanol emulsion membrane system were selected [52–59, Table 2].

The data in Table 3 were calculated similarly to the comparison data, taking into account the most probable kinetic equation (4) [30,31,52–59]:

$$ln\left(C/C_0\right) = -k \cdot K \cdot t = -k_{app} \cdot t \qquad (3.4)$$

where C and C_0 are the concentrations (in mg/L) of pNP at $t=0$ and $t\neq0$, respectively, t being the reaction time, k being the reaction rate constant (mg/(L×min)), K being the adsorption coefficient of the reactant (L/mg), and k_{app} (s^{-1}) being the apparent catalytic rate constant when the concentration (C_0) is very low [60, 61].

The reaction kinetics describe the pNP reduction as a reaction of a pseudo first-order reaction [30,31,60,61].

Catalytic systems based on osmium nanoparticles, coupled with polymer or liquid membranes processes have been less frequently reported [19–21,30,31]. In these hybrid, membrane-catalytic processes, p–nitrophenol is reduced to p–aminophenol with osmium nanoparticles. The hybrid process involves both the conversion of p–nitrophenol in the source phase, and the separation of p–aminophenol, in the receiving phase, through a membrane process. Previously, bulk liquid membranes based on osmium nanoparticles were tested [20,21,30], but also liquid membranes on support (SLM) [19,31].

Table 3.3. Comparative data of the 'apparent catalytic rate constant (k_{app}) in the catalytic reduction reaction of p–nitrophenol to p–aminophenol.

Catalytic material	k_{app} **(s^{-1})**	**Year**	**Refs.**
Os-nanoparticles on Polypropylene hollow fiber membranes	2.04×10^{-4} – 8.05×10^{-4}	2022	[30]
Osmium Nanoparticles/n–Decanol Bulk Membrane	0.8×10^{-4} – 4.9×10^{-4}	2022	[31]
Plasma-enabled synthesis of Pd/GO rich in oxygen-containing groups and defects	13.9×10^{-3}	2022	[52]
Immobilizing of palladium on melamine functionalized magnetic chitosan beads	16.5×10^{-3}	2021	[53]
Ultra-small iridium nanoparticles as active catalysts	5.3×10^{-3}	2020	[54]
Pd@MIL–100(Fe) composite nanoparticles as efficient catalyst	6.5×10^{-3}	2018	[55]
Highly efficient Pd/UiO–66–NH_2 film capillary microreactor	62.3×10^{-3}	2017	[56]
Magnetic nano-porous PtNi/SiO_2 nanofibers	12.84×10^{-3}	2017	[57]
Iridium (0), Platinum (0) and Platinum (0)–Iridium (0) alloy nanoparticles	0.41×10^{-3} (Pt) 0.21×10^{-4} (Ir)	2017	[58]
Iridium oxide nanoparticles and iridium/iridium oxide nanocomposites	2.5×10^{-3} – 5.5×10^{-3}	2015	[59]
Emulsion membranes based on Os–NP/n–decanol or n–dodecanol	0.1×10^{-3} – 0.9×10^{-3}	This work	

The emulsion membrane based on the nanodispersion of osmium in n–decanol or n–dodecanol has superior performance both in the conversion of p–nitrophenol and in the separation of p–aminophenol from the system.

Taking into account relation (3.4), an apparent constant (k_{app}) was obtained, with maximum values between 0.1×10^{-3} s^{-1} for n-dodecanol and 0.9×10^{-3} s^{-1} for n-decanol. These values are about an order of magnitude higher than the other systems with membranes based on osmium nanoparticles previously reported [19,20,30,31], but below the values reported in

the specialized literature, for catalysts based on nanoparticles obtained from the elements platinum group [52–59].

Figure 3.13 shows schematically the hybrid process of catalytic reduction of p–nitrophenol and membrane recovery of p–aminophenol through the new emulsion type membrane.

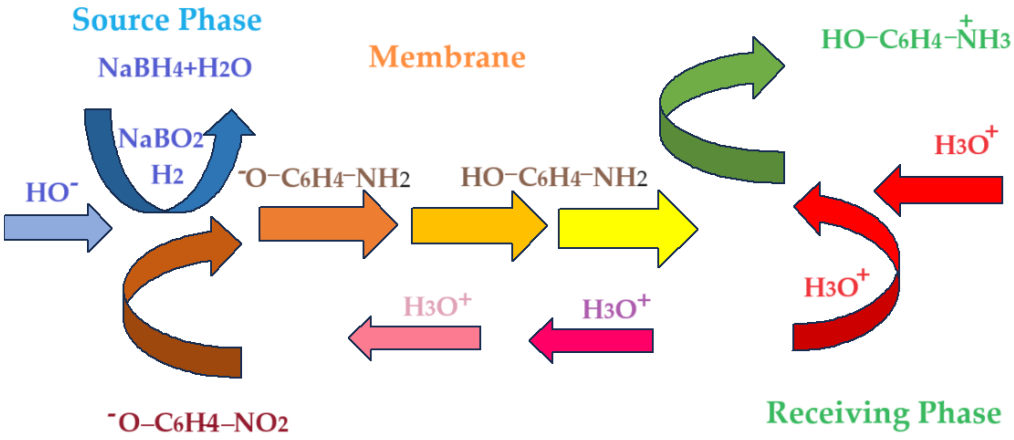

Figure 3.13. Schematic representation of the hybrid process, of p–nitrophenol catalytic reduction and p–aminophenol membrane recovery.

Table 3.4. The main properties of membrane n–alcohols.

Organic compounds	**Molar mass (g/Mol)**	**Solubility in water (g/L)**	**Water solubility (g/L)**	**Viscosity (cP)**	**Relative polarity measure**	**pKa**
n–decanol (nD)	158.28	0.037	0.0211	12.05	−0.540	15.21
n–dodecanol (nDD)	186.34	0.004	0.0019	18.80	−0.511	16.84

For the conversion of p–nitrophenol and the efficiency of p–aminophenol separation according to the scheme in figure 13, the following can be taken into consideration: different molar mass of n–alcohols, mutual solubility of n–alcohols in water and of water in n–alcohols, viscosity, relative polarity and the pKa value (Table 3.4).

Through the proposed mechanism, two interfaces:

- ✓ The source phase/organic phase interface, containing osmium nanoparticles;
- ✓ Organic phase/aqueous receiving phase interface.

and three phases:

- ✓ Aqueous source phase;

- ✓ Organic phase containing osmium nanoparticles;
- ✓ Receiving aqueous phase.

are considered responsible for the conversion of p–nitrophenol and the transport of p–aminophenol in water.

A simplified model of conversion of p–nitrophenol and transport of p–aminophenol involves five steps:

- ✓ Diffusion of p–nitrophenolate and molecular hydrogen from the source aqueous phase to the interface with the catalytic organic phase, due to the content of osmium nanoparticles.
- ✓ Penetration of the source aqueous phase/organic phase interface, simultaneously with the conversion of p–nitrophenolate to p–aminophenol;
- ✓ Diffusion of p–aminophenol across the membrane to the 'organic phase'/'receiving aqueous phase' interface;
- ✓ Penetration of the organic phase/ receiving aqueous phase interface, simultaneously with the reaction of p–aminophenol with the proton;
- ✓ Diffusion of protonated aminophenol in the receiving aqueous phase.

In the proposed model, all the parameters of the working system favor the n–decanol-based membrane (Table 3.3), as follows:

- ✓ The mutual solubility of water in n–alcohols is higher for n–decanol compared to n–dodecanol by almost an order of magnitude;
- ✓ The viscosity of n–decanol is lower by about 30% compared to n–dodecanol.

The two presented aspects lead to friendlier interfaces between the organic phase (n–alcohol) and respectively the two aqueous phases (source and receiver). This means that the interfaces with n–decanol contain more water in n–decanol and more n–decanol in water, favoring the diffusion and penetration of the interface by p–nitrophenol and the source of molecular hydrogen. Of course, the parameters of n–decanol (solubility and viscosity) being an order of magnitude higher than those of n–dodecanol, will disfavor both the conversion of p–nitrophenol and the transport of p–aminophenol.

The proposed model responds to the results presented previously (Figure 3.13), in which the results are better for the membrane containing n–decanol than the one based on n–dodecanol.

From a practical point of view, the only deficiency of n–decanol is that it remains in the aqueous phases at the maximum concentration of 0.037 g/L compared to n–dodecanol of 0.004

g/L. In technological exploitation, this observation leads to the design of a method for the elimination of n–decanol from aqueous effluents. The two n–alcohols with an even number of carbon atoms are biodegradable, which would solve, through bio-degradation, the problem.

Compared to the heterogeneous catalytic systems with solid catalysts, the system with the dispersion of osmium nanoparticles in n–alcohols differ in the type of interface: adsorption in the first case, and absorption in the second. Depending on the nature of the nitroderivative, either heterogeneous adsorption catalysis or heterogeneous absorption catalysis can be favored.

A favorable aspect of the chosen working method would be the reception of p–aminophenol resulting from the reduction of p–nitrophenol in the receiving phase at a concentration 10 times higher. This concentration factor would create the possibility of using the p–aminophenol solution as such in the pharmaceutical or dye industry.

If in terms of reduction, osmium-based membrane systems are inferior to other catalyst systems, it would be interesting for the system to be used in selective oxidation processes.

3.4. Materials and Methods

3.4.1. Reagents and materials

All reagents used in the presented work were of analytical grade. They were purchased from Merck (Merck KGaA, Darmstadt, Germany): osmium tetroxide, sodium hydroxide, hydrochloric acid, $NaBH_4$, p–aminophenol and p–nitrophenol.

The membrane components were purchased from Sigma-Aldrich (Merck KGaA, Darmstadt, Germany): t–butyl alcohol, n–octanol, n–dodecanol, and 10–undecylenic acid (undecenoic acid) have the characteristics presented in Table S1.

The purified water characterized by 18.2 μS/cm conductivity was obtained with a RO Millipore system (MilliQ® Direct 8 RO Water Purification System, Merck, Darmstadt, Germany).

3.4.2. Methods and Procedures

3.4.2.1. Analytical methods

Dynamic light scattering (DLS) analysis [30]: granulometer equipment: Coulter N4 Plus (laser He–Ne, 632.8 nm) (Beckman Coulter GmbH, Krefeld, Deutschland).

For transmission electron microscopy (TEM) using a High-Resolution 80–200 kV Titan THEMIS transmission microscope (Thermo Fisher Scientific, former FEI, Hillsboro, OR,

USA) equipped with an Image Corrector and EDXS detector in the column. The microscope is operated at a 200 kV voltage in transmission mode [30,31].

The scanning electron microscopy studies, SEM and HFSEM, were performed on a Hitachi S4500 system (Hitachi High-Technologies Europe GmbH, Germany) [21,22].

Thermal analysis, TG–DSC was performed with a STA 449C F3 apparatus, from Netzsch (Selb, Germany with a FTIR Tensor 27 from Bruker (Bruker Co., Ettlingen, Germany) [19,20,21].

The UV–Vis studies were performed on dual-beam UV equipment–Varian Cary 50 (Agilent Technologies Inc., Santa Clara, CA, USA.) at a resolution of 1 nm, spectral bandwidth of 1.5 nm, and a scan rate of 300 nm/s. [19].

The UV–Vis validation analysis of the p–nitrophenol solutions was performed on a CamSpec M550 spectrometer (Spectronic CamSpec Ltd., Leeds, UK [21,23].

The electrochemical analysis was followed up with a PARSTAT 2273 Potentiostat (Princeton Applied Research, AMETEK Inc., Oak Ridge, TN, USA) [19,20].

The pH, conductance and anions concentration (in the source phase or in the receiving phase) were determined using a conductance cell or combined selective electrode (HI 4107, Hanna Instruments Ltd., Leighton Buzzard, UK) and a multi-parameter system (HI 5522, Hanna Instruments Ltd., Leighton Buzzard, UK) [19,22].

3.4.2.2. Preparation of nanodispersion of osmium nanoparticles in n–dodecanol and n–dodecanol

The preparation of nanodispersion of osmium nanoparticles in n–decanol was previously presented [30]. Briefly, to obtain the dispersion of osmium nanoparticles, dissolve 1g (0.0039 mol) of osmium tetroxide in 50 mL t–butanol at room temperature, in a 100 mL conical vessel.

Separately, in a 2,000 mL vessel with a hemispherical bottom, introduce 1,250 mL (1,000 g) of n–dodecanol or n–decanol, to which 7.249 g (0.039 mol) of 10–undecylenic acid. After approx. 10 minutes of homogenization, the osmium tetroxide solution is added in drops, when it will be possible to observe the instant formation of an intensely black dispersion. The dispersion obtained (Os–NP/nDD or Os–NP/nD) is washed five times with 200 mL of pure water which is analyzed spectrophotometrically to track the removal of t–butanol or other organic components.

The stability of the prepared nanodispersion is monitored by contacting it with 200 mL of pure water for two weeks, the aqueous layer being analyzed daily spectrophotometrically,

and the osmium dispersion at the water interface with a Motic microscope (MoticEurope, S.L.U., Barcelona, Spain).

3.4.2.3. Preparation of emulsion of acidic aqueous solution (receiving phase) in n–alcohols

A stock emulsion is prepared by intensively mixing 500 mL of osmium dispersion in n–alcohol and 500 mL of acidic aqueous solution. The intense stirring of the immiscible phases is carried out with a propeller type stirrer (Figure S1) with 150 rotations per minute. A black dispersion is obtained whose conductance is lower than that of ultrapure water.

3.4.2.4. Reduction of p–nitrophenol to p–aminophenol

The source phase consisting of a solution of p–nitrophenol 2.78 g/L (2×10^{-2} mol/L) in ultrapure water is mixed with a freshly prepared solution of sodium borohydride 7.566 g/L (0.2 mol/L).

1,000 mL of such a solution is introduced into the 1,500 mL reaction column, and recirculated by means of a peristaltic pump, with a flow rate of 15.0 mL/s. The source solution is recirculated either co-current or counter-currently (Figure 11) with 200 mL of emulsion containing the receiving phase (100 mL) embedded in the osmium nanodispersion in n–alcohols (100 mL). The dispersion of the emulsion containing the receptor phase is carried out with a specific device with the help of the peristaltic pump with a flow rate of 3.5 mL/s.

Monitoring the progress of the reaction is done by taking 1.0 mL of the source solution at predetermined operation interval, then subjected to spectrophotometric determination at λ=404 nm. Calculation of conversion or separation efficiency is done by relations (3) and (4).

3.5. Conclusions

Osmium nanoparticle reaction systems placed on membranes (polymeric or composite) or in bulk membranes have recently been studied to highlight the catalytic characteristics in the reduction reaction of p-nitrophenol to p-aminophenol.

This chapter presents the results of a reaction system with osmium nanoparticles dispersed in n–decanol or n–dodecanol that is constituted in an emulsion type membrane.

The osmium nanoparticles in the membrane dispersion were characterized by SEM, TEM, EDAX, AT (TG and DSC) and the complex analysis of the gases during the thermal decomposition of the dispersion (TA–GC–FTIR). The chemical species taken as the target substance is p–nitrophenol. The source phase of the membrane system consists of p-nitrophenol dissolved in an aqueous solution of sodium borohydride. After reduction in the membrane

phase, the p-aminophenol formed is immobilized as ammonium ion in an acidic receptor solution.

In the proposed system, the flow regime (co-current or counter-current) of the membrane dispersed through the source phase, the pH difference between the source and receiving phases and the number of operating cycles and the nature of the membrane n–alcohol were varied.

The obtained results reveal that the counter-current operation is more advantageous than the co-current operation until a level is reached, which is also given by the co-current flow. In the middle of the working time interval, the counter-current operation is preferred.

The number of reuse cycles of the emulsion membrane is limited by the decrease in conversion. Practically, after five cycles of use, the membrane dispersion must be regenerated. In all experimental cases the conversion results are higher for n–decanol than for n–dodecanol.

Increasing the pH difference between the source and receiving aqueous phases leads to increased conversion. Under the most favorable working conditions, the apparent constant (k_{app} (s^{-1})) is 0.1×10^{-3} for dodecanol and 0.9×10^{-3} for decanol.

REFERENCES

1. Kostanyan, A.E.; Belova, V.V.; Voshkin, A.A. Three- and Multi-Phase Extraction as a Tool for the Implementation of Liquid Membrane Separation Methods in Practice. *Membranes* **2022**, *12*, 926. https://doi.org/10.3390/membranes12100926.
2. Shyam Sunder, G.S.; Adhikari, S.; Rohanifar, A.; Poudel, A.; Kirchhoff, J.R. Evolution of Environmentally Friendly Strategies for Metal Extraction. *Separations* **2020**, *7*, 4. https://doi.org/10.3390/separations7010004.
3. Bóna, Á.; Bakonyi, P.; Galambos, I.; Bélafi-Bakó, K.; Nemestóthy, N. Separation of Volatile Fatty Acids from Model Anaerobic Effluents Using Various Membrane Technologies. *Membranes* **2020**, *10*, 252. https://doi.org/10.3390/membranes10100252.
4. Kostanyan, A.E.; Belova, V.V.; Zakhodyaeva, Y.A.; Voshkin, A.A. Extraction of Copper from Sulfuric Acid Solutions Based on Pseudo-Liquid Membrane Technology. *Membranes* **2023**, *13*, 418. https://doi.org/10.3390/membranes13040418.
5. Aldwaish, M.; Kouki, N.; Algreiby, A.; Tar, H.; Tayeb, R.; Hafiane, A. An Ionic supported liquid membrane for the recovery of bisphenol A from aqueous solution. *Membranes* **2022**, 12, 869. https://doi.org/10.3390/membranes12090869.

6. Khalaf, Z.A.; Hassan, A.A. Studying of the effect of many parameters on a bulk liquid membrane and its opposition in Cd(II) removal from wastewater. *J. Phys. Conf. Ser*. **2021**, 1973, 012097. https://doi.org.10.1088/1742-6596/1973/1/012097.
7. Kárászová, M.; Bourassi, M.; Gaálová, J. Membrane Removal of Emerging Contaminants from Water: Which Kind of Membranes Should We Use? *Membranes* **2020**, *10*, 305. https://doi.org/10.3390/membranes10110305.
8. Li, L.; Ma, G.; Pan, Z.; Zhang, N.; Zhang, Z. Research Progress in Gas Separation Using Hollow Fiber Membrane Contactors. *Membranes* **2020**, *10*, 380. https://doi.org/10.3390/membranes10120380.
9. León, G.; Hidalgo, A.M.; Miguel, B.; Guzmán, M.A. Pertraction of Co(II) through Novel Ultrasound Prepared Supported Liquid Membranes Containing D2EHPA. Optimization and Transport Parameters. *Membranes* **2020**, *10*, 436. https://doi.org/10.3390/membranes10120436.
10. Kim, D.; Nunes, S.P. Green solvents for membrane manufacture: Recent trends and perspectives. *Curr. Opin. Gr. Sustain. Chem.* **2021**, 28, 100427. https://doi.org/10.1016/j.cogsc.2020.100427.
11. Kostanyan, A.E.; Voshkin, A.A.; Belova, V.V.; Zakhodyaeva, Y.A. Modelling and Comparative Analysis of Different Methods of Liquid Membrane Separations. *Membranes* **2023**, *13*, 554. https://doi.org/10.3390/membranes13060554.
12. Atlaskin, A. A.; Kryuchkov, S.S.; Yanbikov, N.R.; Smorodin, K.A.; Petukhov, A.N.; Trubyanov, M.M.; Vorotyntsev, V.M.; Vorotyntsev, I.V. Comprehensive experimental study of acid gases removal process by membrane-assisted gas absorption using imidazolium ionic liquids solutions absorbent, *Sep. Pur. Technol.* **2020**, *239*, 116578. https://doi.org/10.1016/j.seppur.2020.116578.
13. Bazhenov, S.D.; Bildyukevich, A.V.; Volkov, A.V. Gas-liquid hollow fiber membrane contactors for different applications, *Fibers* **2018**, *6*(4), 76; https://doi.org/10.3390/fib6040076.
14. Lee, W.J.; Goh, P.S.; Lau, W.J.; Ismail, A.F.; Hilal, N. Green Approaches for Sustainable Development of Liquid Separation Membrane. *Membranes* **2021**, *11*, 235. https://doi.org/10.3390/membranes11040235.
15. Mulder, M. Basic principles of membrane technology; Kluwer Academic Publishers: A.H. Dordrecht, Netherlands, **1996**; ISBN 0792309782, pp. 340–347.
16. Baker, W. Membrane Technology and Applications, 3rd ed.; John Wiley & SonsLtd., Chichester (UK), ISBN 9780470743720, **2012**, pp. 148–149.

17. León, G.; Hidalgo, A.M.; Gómez, M.; Gómez, E.; Miguel, B. Efficiency, Kinetics and Mechanism of 4-Nitroaniline Removal from Aqueous Solutions by Emulsion Liquid Membranes Using Type 1 Facilitated Transport. *Membranes* **2024**, *14*, 13. https://doi.org/10.3390/membranes14010013.
18. Đurasović, I.; Štefanić, G.; Dražić, G.; Peter, R.; Klencsár, Z.; Marciuš, M.; Jurkin, T.; Ivanda, M.; Stichleutner, S.; Gotić, M. Microwave-Assisted Synthesis of Pt/SnO_2 for the Catalytic Reduction of 4-Nitrophenol to 4-Aminophenol. *Nanomaterials* **2023**, *13*, 2481. https://doi.org/10.3390/nano13172481.
19. Nechifor, A.C.; Goran, A.; Grosu, V.-A.; Pîrțac, A.; Albu, P.C.; Oprea, O.; Grosu, A.R.; Pașcu, D.; Păncescu, F.M.; Nechifor, G.; Tanczos, S.-K.; Bungau, G.S. Reactional Processes on Osmium–Polymeric Membranes for 5–Nitrobenzimidazole Reduction. *Membranes* **2021**, *11*, 633. https://doi.org/10.3390/membranes11080633.
20. Albu, P.C.; Ferencz, A.; Al-Ani, H.N.A.; Tanczos, S.-K.; Oprea, O.; Grosu, V.-A.; Nechifor, G.; Bungău, S.G.; Grosu, A.R.; Goran, A.; Nechifor, A.C. Osmium Recovery as Membrane Nanomaterials through 10–Undecenoic Acid Reduction Method. *Membranes* **2022**, *12*, 51. https://doi.org/10.3390/membranes12010051.
21. Albu, P.C.; Tanczos, S.-K.; Ferencz, A.; Pîrțac, A.; Grosu, A.R.; Pașcu, D.; Grosu, V.-A.; Bungău, C.; Nechifor, A.C. pH and Design on *n*–Alkyl Alcohol Bulk Liquid Membranes for Improving Phenol Derivative Transport and Separation. *Membranes* **2022**, *12*, 365. https://doi.org/10.3390/membranes12040365.
22. Nechifor, G.; Grosu, A.R.; Ferencz, A.; Tanczos, S.-K.; Goran, A.; Grosu, V.-A.; Bungău, S.G.; Păncescu, F.M.; Albu, P.C.; Nechifor, A.C. Simultaneous Release of Silver Ions and 10–Undecenoic Acid from Silver Iron–Oxide Nanoparticles Impregnated Membranes. *Membranes* **2022**, *12*, 557. https://doi.org/10.3390/membranes12060557
23. Ferencz, A.; Grosu, A.R.; Al-Ani, H.N.A.; Nechifor, A.C.; Tanczos, S.-K.; Albu, P.C.; Crăciun, M.E.; Ioan, M.-R.; Grosu, V.-A.; Nechifor, G. Operational Limits of the Bulk Hybrid Liquid Membranes Based on Dispersion Systems. *Membranes* **2022**, *12*, 190. https://doi.org/10.3390/membranes12020190.
24. Bolitho, E.M.; Coverdale, J.P.C.; Bridgewater, H.E.; Clarkson, G.J.; Quinn, P.D.; Sanchez-Cano, C.; Sadler, P.J. Tracking Reactions of Asymmetric Organo-Osmium Transfer Hydrogenation Catalysts in Cancer Cells. *Angew. Chem. Int. Ed*. **2021**, *60*, 6462–6472 International Edition: https://doi.org/10.1002/anie.202016456.
25. Sharpless, K.B.; Amberg, W.; Bennani, Y.L.; Crispino, G.A.; Hartung, J.; Jeong, K.S.; Kwong, H.L.; Morikawa, K.; Wang, Z.M. The osmium-catalyzed asymmetric

dihydroxylation: A new ligand class and a process improvement. *J. Org. Chem*. **1992**, *57*, 10, pp. 2768–2771, https://doi.org/10.1021/jo00036a003.

26. Uribe-Godínez, J.; Castellanos, E.; Borja-Arco, R.H.; Altamirano-Gutiérrez, A.; Jiménez-Sandoval, O. Novel osmium-based electrocatalysts for oxygen reduction and hydrogen oxidation in acid conditions. *J. Power Sources* **2008**, *177*, pp. 286–295, https://doi.org/10.1016/j.jpowsour.2007.11.063.
27. Heller, A. Electron-conducting redox hydrogels: Design, characteristics and synthesis. *Curr. Opin. Chem. Biol*. **2006**, *10*, pp. 664–672. https://doi.org/10.1016/j.cbpa.2006.09.018.
28. Adams, C.W.M.; Abdulla, Y.H.; Bayliss, O.B. Osmium tetroxide as a histochemical and histological reagent. *Histochemie* **1967**, *9*, 68–77, https://doi.org/10.1007/BF00281808.
29. Verma, R; Jaggi, N. A DFT investigation of Osmium decorated single walled carbon nanotubes for hydrogen storage. Interna-tional Journal of Hydrogen Energy 2024. 54, pp. 1507–1520. https://doi.org/10.1016/j.ijhydene.2023.12.110.
30. Nechifor, A.C.; Goran, A.; Tanczos, S.-K.; Păncescu, F.M.; Oprea, O.-C.; Grosu, A.R.; Matei, C.; Grosu, V.-A.; Vasile, B.Ș.; Albu, P.C. Obtaining and Characterizing the Osmium Nanoparticles/*n*–Decanol Bulk Membrane Used for the *p*–Nitrophenol Reduction and Separation System. *Membranes* **2022**, *12*, 1024. https://doi.org/10.3390/membranes12101024.
31. Nechifor, G.; Păncescu, F.M.; Grosu, A.R.; Albu, P.C.; Oprea, O.; Tanczos, S.-K.; Bungău, C.; Grosu, V.-A.; Pîrțac, A.; Nechifor, A.C. Osmium Nanoparticles-Polypropylene Hollow Fiber Membranes Applied in Redox Processes. *Nanomaterials* **2021**, *11*, 2526. https://doi.org/10.3390/nano11102526.
32. Mashentseva, A.A. Effect of the Oxidative Modification and Activation of Templates Based on Poly(ethylene terephthalate) Track-Etched Membranes on the Electroless Deposition of Copper and the Catalytic Properties of Composite Membranes. *Pet. Chem.* **2019**, ***59***, pp. 1337–1344. https://doi.org/10.1134/S0965544119120089
33. Mashentseva, A.A.; Borgekov, D.B.; Niyazova D.T.; Zdorovets, M.V. Evaluation of the catalytic activity of the composite track-etched membranes for *p*-nitrophenol reduction reaction. *Pet. Chem.* **2015**, *55*, pp. 810–815. https://doi.org/10.1134/S0965544115100151.
34. Felix, E.M.; Antoni, M.; Pause, I.; Schaefer, S.; Kunz, U.; Weidler, N.; Muench, F.; Ensinger, W. Template-based synthesis of metallic Pd nanotubes by electroless deposition and their use as catalysts in the 4-nitrophenol model reaction. *Green chemistry*, **2016,** *18*(2), pp. 558–564. DOI: 10.1039/C5GC01356A.

35. Muench, F.; Rauber, M.; Stegmann, C.; Lauterbach, S.; Kunz, U.; Kleebe, H.J.; and Ensinger, W. Ligand-optimized electroless synthesis of silver nanotubes and their activity in the reduction of 4-nitrophenol. *Nanotechnology*, **2011**, *22*(41), p.415602. **DOI:** 10.1088/0957-4484/22/41/415602.
36. Din, M.I.; Khalid, R.; Hussain, Z.; Hussain, T.; Mujahid, A.; Najeeb, J.; Izhar, F. Nanocatalytic assemblies for catalytic reduction of nitrophenols: a critical review. *Critical reviews in analytical chemistry*, **2020**, *50*(4), pp. 322–338. https://doi.org/10.1080/10408347.2019.1637241.
37. Mejía, Y.R.; Bogireddy, N.K.R. Reduction of 4-nitrophenol using green-fabricated metal nanoparticles. *RSC advances*, **2022**, *12*(29), pp. 18661–18675. DOI: 10.1039/D2RA02663E.
38. Elhenawy, S.; Khraisheh, M.; AlMomani, F.; Hassan, M. Key Applications and Potential Limitations of Ionic Liquid Membranes in the Gas Separation Process of CO_2, CH_4, N_2, H_2 or Mixtures of These Gases from Various Gas Streams. *Molecules* **2020**, *25*, 4274. https://doi.org/10.3390/molecules25184274.
39. Von Willingh, G. Recent Advancements in the Development of Osmium Catalysts for Various Oxidation Reactions: A New Era? *Comment Inorg Chem.* **2021**, *41*(5), pp. 249–266. https://doi.org/10.1080/02603594.2021.1888724.
40. Pitto-Barry, A.; Geraki, K.; Horbury, M.D.; Stavros, V.G.; Mosselmans, J.F.W.; Walton, R.I.; Sadler, P.J.; Barry, N.P. Controlled fabrication of osmium nanocrystals by electron, laser and microwave irradiation and characterisation by microfocus X-ray absorption spectroscopy. *Chem Commun (Camb).* **2017**, *53*(96), pp. 12898–12901. DOI: 10.1039/C7CC07133G.
41. Santacruz, L.; Donnici, S.; Granados, A.; Shafir, A. Vallribera, A,Fluoro-tagged osmium and iridium nanoparticles in oxidation reactions. *Tetrahedron.* **2018**; *74*(48), pp. 6890–6895. https://doi.org/10.1016/j.tet.2018.10.040.
42. Hartman, R.L., Flow chemistry remains an opportunity for chemists and chemical engineers. *Current Opinion in Chemical Engineering*, **2020**, *29*, pp. 42–50. https://doi.org/10.1016/j.coche.2020.05.002.
43. Shimoga, G.; Palem, R.R.; Lee, S.-H.; Kim, S.-Y. Catalytic Degradability of *p*-Nitrophenol Using Ecofriendly Silver Nanoparticles. *Metals* **2020**, *10*, 1661. https://doi.org/10.3390/met10121661.
44. Brown, H.K.; El Haskouri, J.; Marcos, M.D.; Ros-Lis, J.V.; Amorós, P.; Úbeda Picot, M.Á.; Pérez-Pla, F. Synthesis and Catalytic Activity for 2, 3, and 4-Nitrophenol Reduction

of Green Catalysts Based on Cu, Ag and Au Nanoparticles Deposited on Polydopamine-Magnetite Porous Supports. *Nanomaterials* **2023**, *13*, 2162. https://doi.org/10.3390/nano13152162.

45. Chen, H.; Yang, M.; Liu, Y.; Yue, J.; Chen, G. Influence of Co_3O_4 Nanostructure Morphology on the Catalytic Degradation of p-Nitrophenol. *Molecules* **2023**, *28*, 7396. https://doi.org/10.3390/molecules28217396.
46. Minisy, I.M.; Taboubi, O.; Hromádková, J. One-Step Accelerated Synthesis of Conducting Polymer/Silver Composites and Their Catalytic Reduction of Cr(VI) Ions and *p*-Nitrophenol. *Polymers* **2023**, *15*, 2366. https://doi.org/10.3390/polym15102366.
47. Da'na, E.; Taha, A.; El-Aassar, M.R. Catalytic Reduction of p-Nitrophenol on MnO_2/Zeolite -13X Prepared with *Lawsonia inermis* Extract as a Stabilizing and Capping Agent. *Nanomaterials* **2023**, *13*, 785. https://doi.org/10.3390/nano13040785.
48. Wang, C.; Zhu, D.; Bi, H.; Zhang, Z.; Zhu, J. Synthesis of Nitrogen and Phosphorus/Sulfur Co-Doped Carbon Xerogels for the Efficient Electrocatalytic Reduction of p-Nitrophenol. *Int. J. Mol. Sci.* **2023**, *24*, 2432. https://doi.org/10.3390/ijms24032432.
49. Zhao, Y.; Yuan, P.; Xu, X.; Yang, J. Removal of *p*-Nitrophenol by Adsorption with 2-Phenylimidazole-Modified ZIF-8. *Molecules* **2023**, *28*, 4195. https://doi.org/10.3390/molecules28104195.
50. Qi, K.; Wang, X.; Liu, S.; Lin, S.; Ma, Y.; Yan, Y. Visible Light Motivated the Photocatalytic Degradation of p-Nitrophenol by Ca^{2+}-Doped $AgInS_2$. *Molecules* **2024**, *29*, 361. https://doi.org/10.3390/molecules29020361.
51. Li, S.; Guo, Y.; Liu, L.; Wang, J.; Zhang, L.; Shi, W.; Aleksandrzak, M.; Chen, X.; Liu, J. Fabrication of FeTCPP@CNNS for Efficient Photocatalytic Performance of p-Nitrophenol under Visible Light. *Catalysts* **2023**, *13*, 732. https://doi.org/10.3390/catal13040732.
52. Zhang, T.; Ouyang, B.; Zhang, X.; Xia, G.; Wang, N.; Ou, H.; Ma, L.; Mao, P.; Ostrikov, K.K.; Di, L.; et al. Plasma-enabled synthesis of Pd/GO rich in oxygen-containing groups and defects for highly efficient 4-nitrophenol reduction. *Appl. Surf. Sci.* **2022**, *4*, 153727. https://doi.org/10.1016/j.apsusc.2022.153727.
53. Wang, G.; Lv, K.; Chen, T.; Chen, Z.; Hu, J. A versatile catalyst for p-nitrophenol reduction and Suzuki reaction in aqueous medium. *Int. J. Biol. Macromol.* **2021**, *184*, pp. 358–368. https://doi.org/10.1016/j.ijbiomac.2021.06.055.
54. Scheuerlein, M.C.; Muench, F.; Kunz, U.; Hellmann, T., Hofmann, J.P.; Ensinger, W. Electroless Nanoplating of Iridium: Template-Assisted Nanotube Deposition for the

Continuous Flow Reduction of 4-Nitrophenol. *ChemElectroChem*, **2020**. 7(16), pp. 3496–3507. https://doi.org/10.1002/celc.202000811.

55. Li, J.; Wu, F.; Lin, L.; Guo, Y.; Liu, H.; Zhang, X. Flow fabrication of a highly efficient Pd/UiO-66-NH2 film capillary microreactor for 4-nitrophenol reduction, *Chem.Eng. J.* **2018**, *333*, pp. 146–152. https://doi.org/10.1016/j.cej.2017.09.154.
56. Xu, B.; Li, X.; Chen, Z.; Zhang, T.; Li, C. Pd@MIL-100(Fe) composite nanoparticles as efficient catalyst for reduction of 2/3/4-nitrophenol: synergistic effect between Pd and MIL-100(Fe), *Microporous Mesoporous Mater*. **2018,** *255*, pp. 1–6, https://doi.org/10.1016/j.micromeso.2017.07.008.
57. Guan, H.; Chao, C.; Kong, W.; Hu, Z.; Zhao, Y.; Yuan, S.; Zhang, B. Magnetic nanoporous PtNi/SiO2 nanofibers for catalytic hydrogenation of p-nitrophenol. *Nanopart Res.* **2017**, *19*, 187. https://doi.org/10.1007/s11051-017-3884-9.
58. Ramírez-Crescencio, F., Redón, R., Herrera-Gomez, A., Gomez-Sosa, G., Bravo-Sanchez, M. and Fernandez-Osorio, A.L., Facile obtaining of Iridium (0), Platinum (0) and Platinum (0)-Iridium (0) alloy nanoparticles and the catalytic reduction of 4-nitrophenol. *Materials Chemistry and Physics*, **2017,** *201*, pp. 289–296. https://doi.org/10.1016/j.matchemphys.2017.08.006.
59. Xu, D.; Diao, P.; Jin, T.; Wu, Q.; Liu, X.; Guo, X.; Gong, H.; Li, F.; Xiang, M.; Ronghai, Y., Iridium oxide nanoparticles and iridium/iridium oxide nanocomposites: photochemical fabrication and application in catalytic reduction of 4-nitrophenol. *ACS Applied Materials & Interfaces*, **2015**, *7*(30), pp. 16738–16749. https://doi.org/10.1021/acsami.5b04504.
60. Bukhamsin, H.A.; Hammud, H.H.; Awada, C.; Prakasam, T. Catalytic Reductive Degradation of 4-Nitrophenol and Methyl orange by Novel Cobalt Oxide Nanocomposites. *Catalysts* **2024**, *14*, 89. https://doi.org/10.3390/catal14010089.
61. Kuźniarska-Biernacka, I.; Ferreira, I.; Monteiro, M.; Santos, A.C.; Valentim, B.; Guedes, A.; Belo, J.H.; Araújo, J.P.; Freire, C.; Peixoto, A.F. Highly Efficient and Magnetically Recyclable Non-Noble Metal Fly Ash-Based Catalysts for 4-Nitrophenol Reduction. *Catalysts* **2024**, *14*, 3. https://doi.org/10.3390/catal14010003.

Part C

General conclusions, originality and perspective of the research

C1. General conclusions

The general objective of the doctoral thesis "Recuperative separation by composite membranes of the compounds involving olfactory discomfort" is the design of membranes and membrane systems for the removing of p-nitrophenol and hydrogen sulfide which generating olfactory discomfort and its recovery.

The specific objectives are:

- Obtaining liquid membranes with osmium nanoparticles
- Preparation of polymeric membranes containing osmium nanoparticles
- Obtaining osmium membrane-nanoparticle composite membranes
- Characterization of the obtained membranes
    - o Scanning electron microscopy (SEM)
    - o Energy dispersive X-ray analysis (EDAX)
    - o Thermo-gravimetric and differential scanning thermal analysis (TG, DSC)
    - o Fourier transform infrared spectroscopy (FTIR)
    - o Spectrometry in the ultraviolet and visible range (UV-Vis)
    - o Dynamic Light Scattering (DLS) analysis.
- Determining the performances of the recuperative separation process.

Chapter 1, Synthesis of the literature data, give as following conclusion:

Among known pollutants, those that cause significant discomfort are those that have a bad smell.

Bad-smelling pollutants are generally also very toxic.

p-nitrophenol belongs to the classes of pollutants with the above characteristics.

Incineration in power plants or through co-incineration in the cement industry leads to unwanted nitrogen oxides.

A recommended procedure for p-nitrophenol is reduction to paminophenol

Catalytic hydrogenation is studied among the reduction processes in this thesis.

For the valorization of p-aminophenol, membrane separation leads to recuperative separation.

The catalytic reduction with molecular hydrogen (NaBH4 in aqueous medium) is intensively studied and the reaction mechanisms are very diverse.

Chapter 2 is**: "**Osmium Nanoparticles–Polypropylene Hollow Fiber Membrane Applied in Redox Processes"

This chapter presented the preparation and characterization of a composite membrane of active metal nanoparticle–polymer support type, based on osmium nanoparticles obtained in situ on a polypropylene hollow fiber membrane. The osmium nanoparticles are generated from a solution of osmium tetroxide of different concentrations in tert–butyl alcohol, by reduction with molecular hydrogen, in a contactor with polypropylene membrane.

The osmium nanoparticles–polypropylene hollow fibers (Os–PP) composite membranes were characterized morphologically and structurally by scanning electron microscopy (SEM), thermal analysis, surface analysis and Fourier Transform Infra-Red (FTIR) spectroscopy.

The performance of osmium nanoparticles–polypropylene hollow fibers (Os–PP2) composite membranes, was tested during the processes of reduction or oxidation of two compounds of technological and biomedical interests (p–nitrophenol and 10–undecylenic acid) from lower saturated alcohol solutions.

The results obtained show that the reduction of p–nitrophenol with molecular hydrogen on composite membranes based on osmium nanoparticles–polypropylene hollow fibers (Os–PP) can be performed with conversions of about 90%, under the following conditions:

- Composite membrane of osmium nanoparticles–polypropylene hollow fibers: Os–PP2 (7,63% atomic Os on the surface),
- Operating time: six hours,
- The concentration p–nitrophenol in t–butanol: 1 g/L,
- Primary alcohol: t–butanol.

Oxidation of 10–undecylenic acid with molecular oxygen on composite membranes of osmium nanoparticles–polypropylene hollow fibers (Os–PP) takes place with conversions of over 80% of solutions in t–butanol of concentration 1–5 g/L, at an operating time of five hours. The composition of the reaction mass to the oxidation of 10-undecylenic acid is complex and requires further studies. Osmium nanoparticle reaction systems placed on membranes (polymeric or composite) or in bulk membranes have recently been studied to highlight the catalytic characteristics in the reduction reaction of p-nitrophenol to p-aminophenol.

Chapter 3 is "Emulsion Liquid Membranes Based on Os–NP/n–decanol or n–dodecanol Nanodispersions for p–Nitrophenol Reduction".

This chapter presents the results of a reaction system with osmium nanoparticles dispersed in n–decanol or n–dodecanol that is constituted in an emulsion type membrane.

The osmium nanoparticles in the membrane dispersion were characterized by SEM, TEM, EDAX, AT (TG and DSC) and the complex analysis of the gases during the thermal decomposition of the dispersion (TA–GC–FTIR). The chemical species taken as the target substance is p–nitrophenol. The source phase of the membrane system consists of p-nitrophenol dissolved in an aqueous solution of sodium borohydride. After reduction in the membrane phase, the p-aminophenol formed is immobilized as ammonium ion in an acidic receptor solution.

In the proposed system, the flow regime (co-current or counter-current) of the membrane dispersed through the source phase, the pH difference between the source and receiving phases and the number of operating cycles and the nature of the membrane n–alcohol were varied.

The obtained results reveal that the counter-current operation is more advantageous than the co-current operation until a level is reached, which is also given by the co-current flow. In the middle of the working time interval, the counter-current operation is preferred.

The number of reuse cycles of the emulsion membrane is limited by the decrease in conversion. Practically, after five cycles of use, the membrane dispersion must be regenerated. In all experimental cases the conversion results are higher for n–decanol than for n–dodecanol.

Increasing the pH difference between the source and receiving aqueous phases leads to increased conversion. Under the most favorable working conditions, the apparent constant (k_{app} (s^{-1})) is 0.1×10^{-3} for dodecanol and 0.9×10^{-3} for decanol.

Chapter 4 is: Reduction of olfactory discomfort in inhabited premises from areas with mofettas through cellulose derivative–polypropylene hollow fiber composite membranes

Treating polluted air with hydrogen sulfide is an important problem for the residential premises in areas with mofettas or extinct volcanoes.

This chapter presents the results of hydrogen sulphide removal from an enclosure with a defined volume using cellulose derivative-polypropylene hollow fiber composite membranes. All membranes obtained were characterized by SEM, EDAX, FTIR, 2D FTIR maps and thermal analysis (TG, DSC). Among the four prepared membranes: sodium carboxymethyl-cellulose–polypropylene hollow fiber (P1), cellulose acetate–polypropylene hollow fiber (P2), methyl 2–

hydroxyethyl-cellulose–polypropylene hollow fiber (P3), and 2–hydroxyethyl-cellulose–polypropylene hollow fiber (P4) the best results of hydrogen sulfide pertraction and capture in a receiving phase of cadmium nitrate solution were obtained with the composite membrane P1.

The optimal operating conditions are: flow rate of 50 L/min of air polluted with 20 ppm hydrogen sulphide, pH between 2 and 4 for the receiving phase of cadmium nitrate of concentration 0.1 mol/L.

The membrane covered with cadmium sulfide is recommended for heat treatment (melting) and obtaining reflective material for road markings.

C2. Originality

In the doctoral thesis, "Recuperative separation by composite membranes of the compounds involving olfactory discomfort", the following original results were obtained:

Preparation of polymer composite membranes – osmium nanoparticles:

- Polypropylene - osmium nanoparticles.
- Cellulose acetate - osmium nanoparticles.
- Polysulfone - osmium nanoparticles.

Obtaining n-alcohol composite membranes - osmium nanoparticles.

Preparation of polymer composite membranes cellulose derivatives-polypropylene hollow fiber.

Catalytic reduction of p-nitrophenol with the membrane classes obtained.

Determining the performance of membranes in the process of catalytic reduction of p-nitrophenol to p-aminophenol.

Recuperative separation of p-aminophenol by composite membranes.

Recuperative separation of hydrogen sulfide.

C3. Perspective of the research

The results obtained in the PhD thesis **"Recuperative separation by composite membranes of the compounds involving olfactory discomfort",** allow obtaining new types of composite membranes based on osmium nanoparticles.

Composite membranes based on osmium nanoparticles can be used to reduce or oxidize a wide range of organic compounds

The thesis "Recuperative separation by composite membranes of the compounds involving olfactory discomfort", fulfilled both its general objective and specific objectives, being validated by six ISI articles with an impact factor above the value of 3.

Andreia PÎRȚAC publication list

1. **Pîrțac, A.**, Nechifor, A.C., Tanczos, S.-K., Oprea, O.C., Grosu, A.R., Matei, C., Grosu, V.-A., Vasile, B.Ú., Albu, P.C., Nechifor, G.
Emulsion Liquid Membranes Based on Os–NP/n–Decanol or n–Dodecanol Nanodispersions for p–Nitrophenol Reduction
(2024) *Molecules*, 29 (8), art. no. 1842. **FI=4,2.**
DOI: 10.3390/molecules29081842

2. Albu, P.C.; **Pîrțac, A.**; Motelica, L.; Nechifor, A.C.; Man, G.T.; Grosu, A.R.; Tanczos, S.-K.; Grosu, V.-A.; Nechifor, G. Reduction in Olfactory Discomfort in Inhabited Premises from Areas with Mofettas through Cellulosic Derivative–Polypropylene Hollow Fiber Composite Membranes. *Materials* **2024**, *17*, 4437. **FI=3,1.**
https://doi.org/10.3390/ma17174437

3. Albu, P.C., Tanczos, S.-K., Ferencz, A., **Pîrțac, A.**, Grosu, A.R., Pașcu, D., Grosu, V.-A., Bungău, C., Nechifor, A.C.
pH and Design on n–Alkyl Alcohol Bulk Liquid Membranes for Improving Phenol Derivative Transport and Separation
(2022) *Membranes*, 12 (4), art. no. 365, **FI=3,3.**
DOI: 10.3390/membranes12040365

4. Nechifor, G., Păncescu, F.M., Grosu, A.R., Albu, P.C., Oprea, O., Tanczos, S.-K., Bungău, C., Grosu, V.-A., **Pîrțac, A.**, Nechifor, A.C.
Osmium nanoparticles-polypropylene hollow fiber membranes applied in redox processes
(2021) *Nanomaterials*, 11 (10), art. no. 2526, **FI=4,4.**
DOI: 10.3390/nano11102526

5. Nechifor, A.C., Goran, A., Grosu, V.-A., **Pîrțac, A.**, Albu, P.C., Oprea, O., Grosu, A.R., Pașcu, D., Păncescu, F.M., Nechifor, G., Tanczos, S.-K., Bungău, S.G.
Reactional processes on osmium–polymeric membranes for 5–nitrobenzimidazole reduction
(2021) *Membranes,* 11 (8), art. no. 633, **FI=3,3.**
DOI: 10.3390/membranes11080633

6. Nechifor, A.C., **Pîrțac, A.**, Albu, P.C., Grosu, A.R., Dumitru, F., Dimulescu, I.A., Oprea, O., Pașcu, D., Nechifor, G., Bungău, S.G.
Recuperative amino acids separation through cellulose derivative membranes with microporous polypropylene fiber matrix
(2021) *Membranes*, 11 (6), art. no. 429, **FI=3,3.**
DOI: 10.3390/membranes11060429

7. Nechifor, A.C., Cotorcea, S., Bungău, C., Albu, P.C., Pașcu, D., Oprea, O., Grosu, A.R., **Pîrțac, A.**, Nechifor, G.
Removing of the sulfur compounds by impregnated polypropylene fibers with silver nanoparticles-cellulose derivatives for air odor correction
(2021) *Membranes*, 11 (4), art. no. 256, **FI=3,3.**
DOI: 10.3390/membranes11040256

8. Cotorcea, S., Dimulescu, I.A., Pașcu, D., Bărdacă, C., Nechifor, G., **Pîrțac, A.**
Membranes based on cellulose acetate recovered from cinematographic films for protein retention
(2021) UPB Scientific Bulletin, Series B: Chemistry and Materials Science, 83 (4), pp. 43-54.